Structure and Vibrations of Lanthanide Trihalides: An Assessment of Experimental and Theoretical Data

Attila Kovács[a) and Rudy J. M. Konings[b)

European Commission, Joint Research Centre, Institute for Transuranium Elements,
P.O. Box 2340, 76125 Karlsruhe, Germany

In the present paper an assessment of experimental and theoretical data on the structure and molecular vibrations of all the LnX_3 lanthanide trihalides (X=F,Cl,Br,I) is presented. Our review includes 114 references to recent advanced studies. These data facilitated the confirmation of previously suggested trends in the molecular properties of the title compounds and a reliable estimation of the data of less-studied LnX_3 molecules. On the basis of the collected data, a comparative analysis of the experimental and computational results has been performed. This served to assess the capabilities of recent theoretical methods for the above molecular properties. © *2004 American Institute of Physics.* [DOI: 10.1063/1.1595651]

Key words: lanthanide trihalides, molecular geometry, molecular vibrations, quantum chemical calculations.

Contents

[a)]Permanent address: Research Group for Technical Analytical Chemistry of the Hungarian Academy of Sciences, Institute of General and Analytical Chemistry, Budapest University of Technology and Economics, H-1521 Budapest, Hungary.
[b)]Author to whom correspondence should be addressed; electronic mail: konings@itu.fzk.de

1. Introduction

Knowledge of the molecular parameters of polyatomic gaseous species is essential for the calculation of their thermodynamic functions. Such calculations are generally made for the ideal gas state using standard statistical thermodynamic equations[1] that relate the heat capacity (and hence the entropy and enthalpy) to the molecular partition function Q. This function is composed of translation, electronic, vibration and rotation components, which can be treated independently (Born–Oppenheimer approximation). The translation component is calculated from the molecular weight of the molecule, the electronic component from the molecular energy levels, which are often derived from the free metal ion levels. The rotation component is calculated from the moment of inertia of the molecule, which is derived from the molecular structure; the vibration contribution is derived from the fundamental frequencies of the molecule.

Such an approach is applied in the NIST–JANAF Thermochemical Tables for many inorganic and organic compounds.[2] These tables do not include the lanthanide compounds, which have found interesting technological applications.[3,4] The trihalides are of particular interest in the nuclear[5] and lighting industry,[6] which involve high-temperature processes that can be represented adequately by thermochemical models to design and optimize new products and technological routes. The thermodynamic functions of the gaseous lanthanide trihalides (LnX$_3$) were calculated systematically by Myers and Graves[7] in 1977 and this work is still the most frequently cited reference. The calculations were mainly based on structural and vibrational parameters estimated empirically, as experimental data were very limited at that time.

In the past decade the structure and vibrational spectra of lanthanide trihalides have been studied extensively leading to a wealth of new information. Development in both the experimental and theoretical methods resulted in data of considerably improved accuracy with respect to those obtained before. Many early experimental data have been reanalyzed, and several computations have been performed on some "popular" LnX$_3$ species. As a consequence, a considerable amount of structural and vibrational data is now available facilitating: (i) an evaluation of trends in the various properties and estimation of the missing data of the non- or less-investigated molecules as well as (ii) the assessment of the strengths and weaknesses of current computational methods.

Compilations of the geometrical properties of LnX$_3$ halides have been included in several reviews on metal halides. A comprehensive collection of the experimental structural data is included in Volume II/25 of the Landolt–Börnstein

series[8] in 1998 whereas the experimental and selected theoretical results have been reviewed in 2000 by Hargittai.[9] The latter review focused on the well-defined experimental r_g parameters of thermally averaged structures. However, in several cases, e.g., in thermodynamic and theoretical studies, the equilibrium geometrical parameters would be required. On the other hand, a comprehensive summary of recent results on the vibrational properties is not available. The vibrational frequencies of some lanthanide trihalides appear in compilations of Papatheodorou (1983[10] and 1996[11]) and in that of Zasorin (1989[12]) based on the early experimental studies.

The goal of the present paper is to provide a complete collection of reliable experimental data on the molecular geometry and molecular vibrations of lanthanide trihalides focussing on the equilibrium geometrical parameters and unperturbed (gas-phase) molecular vibrations. The experimental data are critically analyzed and trends in the various properties are evaluated. We compile all recent theoretical results on the structural and vibrational properties of LnX$_3$ compounds and assess the capabilities of current standard theoretical methods. On the basis of the collected data and evaluated trends we provide "recommended values" for geometrical and vibrational parameters of the LnX$_3$ molecules. This data set is recommended for the calculation of the thermodynamic properties and is suggested as reference for theoretical computations. Furthermore, our study should provide a guide for new experimental measurements.

2. Methods for Structural Studies of LnX$_3$ Compounds

2.1. Gas Electron Diffraction (ED)

Among the experimental techniques for gas-phase structure determination the electron diffraction method is the best suited for lanthanide trihalides. Due to the high symmetry (pyramidal C_{3v} or planar D_{3h}) of these molecules their radial distribution curves contain only two peaks which can be attributed to the Ln–X and X$\cdots$X intramolecular distances. This would imply a straightforward interpretation. However, the accuracy of the ED results depends also on a few additional factors.[9]

(i) High-temperature effects: The high vaporization temperatures of LnX$_3$ compounds lead to an enhanced population of the higher vibrational states of these floppy molecules, especially those of the low-frequency bending fundamentals. Due to the large vibrational amplitudes the measured thermal-average geometry may differ considerably from the equilibrium one. The best-known consequence of thermal vibrations is the shrinkage effect leading to smaller bond angles.[13] In the case of a planar MX$_3$ molecule this indicates erroneously a pyramidal structure.

(ii) Anharmonicity of molecular vibrations: This factor has been often neglected in the past. The disadvantages of the harmonic model have been discussed in the literature[9,14] and it is difficult to quantify the effects.

(iii) Dimers: Dimers can be present in the vapor of LnX_3 compounds up to 20%.[9,15–20] Some of their Ln···X and X···X distances are close to those of the monomers resulting in a complex scattering pattern in the experiment. Ignoring the dimer content in the data analysis generally leads to overestimation of the Ln–X bond distances and underestimation of the X–Ln–X angles. The dimers are discussed in Sec. 5.

In recent years considerable progress in the ED technique could be observed, particularly by introduction of auxiliary results in the structure analysis. Mass spectrometric measurements under similar experimental conditions can help in identifying the species present in the vapor.[19–21] Advanced quantum chemical computations can give information on the differences of bond lengths of the target and other related species present in the vapor as well as on the bending and puckering potential curves of these molecules. By means of the potential function the thermal average structure can be described by a series of model conformers in a so-called "dynamic analysis" solving the problem of large amplitude vibrations. Spectroscopic (SP) experiments aid the electron diffraction analysis by providing accurate vibrational data for calculation of vibrational amplitudes. In order to determine the equilibrium geometrical parameters, a joint ED/SP method has been developed for a few simple molecular types.[22–24] Presently, such advanced ED studies of LnX_3 compounds are in progress by Professor Girichev at the Ivanovo State University, by Professor Ezhov at the United Institute of High Temperatures (Russia), and by Professor Hargittai at the Eötvös University (Hungary).

In the forthcoming discussion the following types of geometrical parameters will be used: The distance between equilibrium nuclear positions, "r_e," corresponding to the minimum of the potential energy surface. It is the result of any non-constrained quantum chemical geometry optimization. The thermal average internuclear distance, "r_g," is the distance averaged over molecular vibrations. The final results of ED analysis generally refer to this quantity.

2.2. Vibrational Spectroscopy

Infrared (IR) and Raman spectroscopy are the primary tools for determination of the fundamental frequencies of molecules. They can be applied to gas-phase and matrix-isolated (MI) species. Because the selection rules are different for the C_{3v} and D_{3h} symmetries (cf. Sec. 4.1), vibrational spectroscopy can also give information on the molecular symmetry. This property is important in the calculation of the entropy, as the symmetry number is different for the two types: 3 and 6 for C_{3v} and D_{3h}, respectively.

Because of the extremely high evaporation temperatures, gas-phase studies on LnX_3 compounds need specially devised equipment. The most crucial factors are the high-temperature gas-cell and the sensitivity in the low-wavenumber range. Early studies prior the Fourier transform-infrared (FT-IR) technique[25,26] suffered especially from the latter limitation. Recently, gas-phase FT-IR measurements on selected LnX_3 compounds have been per-

formed down to 25 cm^{-1}.[27–30] They provided the first (and hitherto only) gas-phase experimental information on the low-wavenumber bending fundamentals of lanthanide trihalides. For a few compounds the FT-IR studies have been extended with Raman experiments on the matrix-isolated species giving unambiguous experimental data on the ν_1 fundamentals.[30,31]

The interpretation of the experimental vibrational spectra, however, is not free from difficulties. The high temperatures result in extensively broadened bands in the gas-phase spectra due to the considerably populated higher rotational and vibrational levels. The superposition of the complex rotational envelope with hot bands makes the localization of the band origin uncertain and the identification of the weak ν_1 band near the intense asymmetric stretching (ν_3) band ambiguous. Another effect of the broadening can be the masking of weak fundamental bands by the noise and an uncertain determination of the bending frequencies near the low-detection limit of the spectrometers. MI spectroscopy is made at very low temperatures giving sharp bands. This technique has, however, the problem of matrix-shifts and splitting effects and possible changes in the molecular symmetry due to ion-induced-dipole interactions with the matrix.[32] Additionally, the "cage effect" of the matrix should be noted: under MI conditions the formation of dimers is enhanced whereas these could not be detected in the gas-phase IR spectra of any LnX_3 compound.

2.3. Quantum Chemical Computations

During the past decade, computations have become feasible for a large group of chemical compounds. The progress is due to the revolutionary increase in the technical performance, the release (and continuous improvement) of user-friendly software packages and the development of new computational methods, like density functional theory (DFT). With these increased capabilities, computational chemistry has become an alternative for experimental techniques in several fields of chemistry. Theoretical methods are especially attractive for systems that are difficult to prepare and have too low vapor pressures or limited stability for experimental investigations.

The theoretical background of quantum chemical calculations on lanthanide systems has been discussed in detail by Dolg.[33,34] In the following we focus on some general points.

In the computation of heavy metal halides the key step was the evaluation of relativistic effective core potentials (ECPs). They have the advantage of the reduced basis set size by treating the chemically inert core electrons by a simple potential and incorporating the (for this class of compounds) indispensable relativistic effects. The following ECPs have found application in the structural studies of lanthanide trihalides:

(i) The energy-consistent quasirelativistic ECPs of Dolg et al.[35,36] with contracted $[5s4p3d]$ valence basis sets for the lanthanides. These potentials (denoted as ECP_D in the following) are available for the complete lanthanide series

and include the f electrons in the core. This approximation is reasoned by the fact, that the $4f$ orbitals of the Ln(III) ions are located well below the valence shell with radial maxima at around 50 pm. (The tail of the $4f$ orbitals beyond 200 pm can be important in terms of spectroscopic and magnetic properties, but is considered to be insignificant as far as accurately predicting geometries.[37]) The advantage of ECP_D from a technical point of view is that the lanthanide trihalides can be treated as closed-shell systems which is computationally less demanding. It should be noted that there are new small core lanthanide ECPs of the Stuttgart group including the $4f$ electrons in the valence basis.[38–41] These ECPs, however, have not found application in LnX_3 structural research hitherto.

(ii) The relativistic ECPs of Stevens *et al.*[37] (ECP_S) include the f electrons in the valence shell. The valence basis has the contraction scheme of $[4s4p3d]$ for La,[42] while $[4s4p2d2f]$ for the other lanthanides.[37] Except for LaX_3 and LuX_3 the lanthanide trihalides are open-shell systems in terms of ECP_S leading to technical difficulties when using less-suited programs.

(iii) The relativistic ECP of Hay and Wadt[43] (ECP_{HW}) is available only for lanthanum among the lanthanides which limited its application. The $[3s3p2d]$ contracted valence basis set is relatively small, but gave results comparable to those of ECP_D and ECP_S.

In addition to ECPs, the relativistic effects can be taken into account directly in the computations. Among such codes the Amsterdam Density Functional (ADF) package[44] has found application in LnX_3 research.[45] It contains the relativistic Dirac–Slater method coupled to various DFT functionals. The all-electron basis sets of ADF (up to polarized quadruple-zeta quality) consist of Slater functions.[46]

Another important factor in the computation of metal halides is the proper treatment of electron correlation. Methods used most extensively are the second order Møller–Plesset (MP2) perturbation[47] and various DFT models.[48,49] The most popular Becke3–Lee–Yang–Parr (B3LYP)[50,51] and Becke3–Perdew86 (B3P)[50,52] DFT methods perform in general similarly to MP2.[53] Studies of lanthanide trihalides using more sophisticated levels of theory, like coupled-cluster with single double triple excitations (CCSD(T)), have not been reported hitherto.

Unfortunately, an overall assessment of the theoretical methods for metal halides (including lanthanide compounds) has been hampered by the lack of accurate experimental data and the relatively scarce experience accumulated on the computation of such molecules. The large variety of theoretical levels led to various computations on individual or a small set of compounds, lacking in this way consistency and minimizing the chance to evaluate systematic errors. Nevertheless, from the available results it is clear that the quality of the computed data on metal halides does not reach the usually excellent performance on common organic molecules. It may be partly understood by the huge number of different elements the inorganic compounds are built from, where each element, or group of elements, has its own unique

bonding peculiarities. The computation of heavy compounds seems to suffer in a larger extent from the approximations in the basis sets and the treatment of electron correlation and relativistic effects.

3. Geometry

In this section we assess the available experimental and theoretical data on the molecular geometry of LnX_3 compounds. Unlike previous related studies, we focus here on the r_e experimental data comparing them with computed (r_e) geometries. As pointed out by Hargittai,[54] a comparison of r_g experimental parameters with computed (r_e) ones suffers from the difference in their physical meaning. A seemingly good agreement was often interpreted for the favor of the computations[45,55] although there are several pm differences between r_g and r_e bond distances. It applies even more to the molecular shape because of the significant effects of thermal vibrations on the bond angles.

3.1. Experimental Studies

Most of the available experimental r_e geometries in Tables 1–4 originate from a recent study of Zasorin.[56] He reanalyzed early experimental measurements on 13 lanthanide trihalides in terms of equilibrium structure parameters using estimated vibrational force fields. Deficiencies of his work are the neglect of a possible dimer content in the gaseous phase and the harmonic approximation at the evaluation of the structural (both r_g and r_e) parameters. Recent ED studies on $LuCl_3$,[19] $ErBr_3$,[20] $DyBr_3$,[9] CeI_3,[17] and DyI_3[9] indicated 3%–20% dimer in the high temperature vapors. Neglect of the dimer content leads to overestimated Ln–X bond distances and underestimated X–Ln–X bond angles.[9,57] Based on a large number of studies on metal halides an effect of ∼1 pm Ln–X bond lengthening upon each percentage of (neglected) dimer content was suggested.[9] Recent studies on $LuCl_3$[19] and $ErBr_3$[20] reported a somewhat smaller effect. In fact, parallel studies on $GdCl_3$ and $LuCl_3$ that took carefully into account the dimer contribution resulted in shorter r_g bond distances than those of Zasorin (cf. Table 2). This suggests slightly overestimated Ln–X bond distances and underestimated X–Ln–X angles by Zasorin.[56] On the other hand, the neglect of anharmonicity of the stretching vibrations acts in the opposite direction[9] thus may (partly) compensate for the neglect of dimer. Because of the lack of sufficient information the exact impact of anharmonicity on the r_g parameters is difficult to assess.

A determination of the equilibrium structure of LnX_3 compounds from r_g ED results requires the knowledge of the vibrational force field of the molecules. In past studies, due to a lack of gas-phase data, this was obtained primarily on the basis of IR/MI or estimated frequencies. Moreover, various approximation procedures for evaluation of the equilibrium bond distance have been suggested.[13,14,24] The results obtained by the different methods differ by a few pm from each other.[18] All these facts imply a larger uncertainty for the ED geometrical parameters than the experimental errors given in most original studies.

TABLE 1. Structural parameters [bond distances (pm) and bond angles (deg)] and vibrational frequencies (cm^{-1}) of the lanthanide trifluorides

LnF_3	Reference	Method[a]	La–X	X–La–X	Fundamentals			
					ν_1	ν_2	ν_3	ν_4
LaF_3	Hargittai[54]	ED/gas (r_α)	213(6)					
	Wesley and DeKock[99]	IR/MI(Ar)				84	478	120
		IR/MI(Kr)					474	
		IR/MI(N_2)				84	457	116
	Hastie et al.[93]	IR/MI(Ne)			527.9	81	496.6	130
		IR/MI(Ar)			513.0	83	479.0	121.1
		IR/MI(N_2)			490	94	459	112
		IR/gas (estimated)			540(10)	82(10)	510(10)	125(10)
	Dolg et al.[70]	QC(CISD+Q/ECP_Df,ECP_Dd)	215.9	120.0				
	Adamo and Maldivi[72]	QC(B3LYP/ECP_Sf,ECP_Sd)	216.1	115.1	527	83	512	131
	Adamo and Maldivi[45]	QC(BP-DS/TZ,TZd)	212.4	114.8	521	63	496	113
		QC(B3P/ECP_Sf,ECP_Sd)	217.7	115.4	517	83	485	127
		QC(BP/ECP_Sf,ECP_Sd)	216.8	112.7				
	Joubert et al.[114]	QC(B3LYP/ECP_D,VDZd)	214	110.8	553	88	538	117
	Joubert et al.[55]	QC(MP2/ECP_D,VDZd)	215	112.9	554	72	539	114
	Vetere et al.[74]	QC(PBE/ECP_Sf,ECP_Sd)	215.8	114.0	527	78	516	124
		QC(PBE0/ECP_Sf,ECP_Sd)	214.9	115.6	539	65	529	126
		QC(PBE0/ECP_S,VDZd)	213.3	114.4				
	Adamo and Barone[73]	QC(PBE0/ECP_D,ECP_Dd)	217.4	113.9	532	76	522	119
		QC(PBE0/ECP_D,VTZd)	216.7	113.5				
		QC(PBE0/ECP_S,ECP_Sd)	217.7	114.1	531	77	519	131
		QC(PBE0/ECP_S,VTZd)	217.2	114.5				
	Kovács[77]	QC(B3P/$ECP_D2\,fg$,VTZ2df)	212.9	114.4				
		QC(B3P/ECP_D,VTZd)	217.1	113.8	526	75	515	120
	Solomonik and Marochko[82]	QC(MP2/ECP_S3f,ECP_Sd)	212.7	116.5	535	54	512	117
		QC(CISD+Q/ECP_S3f,ECP_Sd)	212.9	117.5	535	46	511	120
CeF_3	Wesley and DeKock[99]	IR/MI(Ar)				86	483	
		IR/MI(Kr)					479	
		IR/MI(N_2)				86	465	116
	Hastie et al.[93]	IR/MI(Ne)			536.9	78	505.3	
		IR/MI(Ar)			521.5	94	488.3	134
		IR/MI(N_2)			506	82	468	121
		IR/gas (estimated)			549(8)	80(15)	519(8)	115(15)
	Dolg et al.[70]	QC(CISD+Q/ECP_Df,ECP_Dd)	214.0	120.0				
	Cundari et al.[69]	QC(MCSCF/ECP_S,ECP_Sd)	214	120.0				
	Lanza and Fragala[115]	QC(MP2/ECP_S,VDZd)	208.0	112.7				
		QC(MP2/ECP_S,TZ2d)	211.5	117.1				
	Joubert et al.[55]	QC(MP2/ECP_D,VDZd)	213	113.7	558	68	544	115
PrF_3	Zasorin[56]	ED/gas (r_g)	209.1(3)	102.6(28)				
		ED/gas (r_e)	205.6(5)	105.0(15)				
	Wesley and DeKock[99]	IR/MI(Ar)			542[b]	86	458[b]	99
		IR/MI(Kr)			538[b]		455[b]	
		IR/MI(N_2)				86	488	118
	Lesiecki et al.[31]	Raman/MI(Ar)			526		458[b]	99
		IR/MI(Ar)				86	458[b]	99
	Dolg et al.[70]	QC(CISD+Q/ECP_Df,ECP_Dd)	212.6	120.0				
	Cundari et al.[69]	QC(MCSCF/ECP_S,ECP_Sd)	212	120.0				
	Joubert et al.[55]	QC(MP2/ECP_D,VDZd)	212	114.1	562	65	548	117
NdF_3	Wesley and DeKock[99]	IR/MI(Ar)				86	502	118
		IR/MI(Kr)					499	
		IR/MI(N_2)				86	482	123
	Hastie et al.[93]	IR/MI(Ne)			544.9	81	521.4	121
		IR/MI(Ar)			529.7	87	503.7	119
		IR/MI(N_2)			505	103	483	124
		IR/gas (estimated)			557(10)	80(15)	535(10)	115(15)
	Dolg et al.[70]	QC(CISD+Q/ECP_Df,ECP_Dd)	211.1	120.0				
	Cundari et al.[69]	QC(MCSCF/ECP_S,ECP_Sd)	211	120.0				
	Joubert et al.[55]	QC(MP2/ECP_D,VDZd)	210	114.6	566	63	553	118

TABLE 1. Structural parameters [bond distances (pm) and bond angles (deg)] and vibrational frequencies (cm^{-1}) of the lanthanide trifluorides—Continued

LnF$_3$	Reference	Method[a]	La–X	X–La–X	Fundamentals			
					ν_1	ν_2	ν_3	ν_4
PmF$_3$	Dolg et al.[70]	QC(CISD+Q/ECP$_D f$,ECP$_D d$)	210.4	120.0				
	Cundari et al.[69]	QC(MCSCF/ECP$_S$,ECP$_S d$)	210	120.0				
	Joubert et al.[55]	QC(MP2/ECP$_D$,VDZd)	209	115.5				
SmF$_3$	Wesley and DeKock[99]	IR/MI(Ar)				92	508	123
		IR/MI(Kr)					504	
		IR/MI(N$_2$)					491	
	Dolg et al.[70]	QC(CISD+Q/ECP$_D f$,ECP$_D d$)	208.4	120.0				
	Cundari et al.[69]	QC(MCSCF/ECP$_S$,ECP$_S d$)	208	120.0				
	Joubert et al.[55]	QC(MP2/ECP$_D$,VDZd)	208	116.3	571	50	557	119
EuF$_3$	Wesley and DeKock[99]	IR/MI(Ar)				94	511	124
		IR/MI(Kr)					507	
		IR/MI(N$_2$)					502	
	Hastie et al.[93]	IR/MI(Ne)			557.5	89	529.5	133
		IR/MI(Ar)			542.4	94.0	511.7	127
		IR/MI(N$_2$)			532	101	504	120
		IR/gas (estimated)			572(10)	90(15)	544(10)	120(10)
	Dolg et al.[70]	QC(CISD+Q/ECP$_D f$,ECP$_D d$)	206.9	120.0				
	Cundari et al.[69]	QC(MCSCF/ECP$_S$,ECP$_S d$)	207	120.0				
	Joubert et al.[55]	QC(MP2/ECP$_D$,VDZd)	206	118.3	579	37	571	122
GdF$_3$	Zasorin[56]	ED/gas (r_g)	205.3(3)	108.4(24)				
		ED/gas (r_e)	201.6(6)	109.9(23)				
	Hastie et al.[93]	IR/MI(Ne)			560.2	94	537.3	138
		IR/MI(Ar)			544.7	100	519.2	133
		IR/MI(N$_2$)			532	116	500	143
		IR/gas (estimated)			583(10)	95(15)	552(10)	130(10)
	Dolg et al.[70]	QC(CISD+Q/ECP$_D f$,ECP$_D d$)	205.6	120.0				
	Cundari et al.[69]	QC(MCSCF/ECP$_S$,ECP$_S d$)	206	120.0				
	Lanza and Fragala[71]	QC(CAS-MCSCF/ECP$_S$,VDZd)	204.7	119.9	577	116	568	134
		QC(MP2/ECP$_S$,VDZd)	202.0	115.2				
		QC(MP2/ECP$_S$,TZ2d)	204.8	118.9				
	Adamo and Maldivi[72]	QC(B3LYP/ECP$_S$,ECP$_S d$)	205.6	117.7	569	119	553	138
	Adamo and Maldivi[45]	QC(BP-DS/TZ,TZd)	203.1	113.9	563	48	549	138
		QC(B3P/ECP$_S$,ECP$_S d$)	205.0	117.5	569	117	553	138
		QC(BP/ECP$_S$,ECP$_S d$)	204.6	115.6				
	Joubert et al.[114]	QC(B3LYP/ECP$_D$,VDZd)	204	113.6	581	58	564	125
	Joubert et al.[55]	QC(MP2/ECP$_D$,VDZd)	206	117.8	575	39	564	121
	Vetere et al.[74]	QC(PBE/ECP$_S$,ECP$_S d$)	204.6	114.5	562	67	543	138
		QC(PBE0/ECP$_S$,VDZd)	201.5	114.2				
	Adamo and Barone[73]	QC(PBE0/ECP$_D$,ECP$_D d$)	205.8	117.0	555	57	537	136
		QC(PBE0/ECP$_D$,VTZd)	205.5	117.4				
		QC(PBE0/ECP$_S$,ECP$_S d$)	205.6	117.6	577	55	560	139
		QC(PBE0/ECP$_S$,VTZd)	205.3	117.7				
TbF$_3$	Hauge et al.[92]	IR/MI(Ne)			566.7		540.1	
		IR/MI(Ar)			551.1		523.1	
		IR/MI(N$_2$)					509	
	Dolg et al.[70]	QC(CISD+Q/ECP$_D f$,ECP$_D d$)	204.3	120.0				
	Cundari et al.[69]	QC(MCSCF/ECP$_S$,ECP$_S d$)	205	120.0				
	Joubert et al.[55]	QC(MP2/ECP$_D$,VDZd)	205	119.1	576	24	566	121
DyF$_3$	Bencze et al.[94]	IR/MI(Ar)			554.4		531.6	
		IR/MI(N$_2$)			540.2		513	
	Dolg et al.[70]	QC(CISD+Q/ECP$_D f$,ECP$_D d$)	203.0	120.0				
	Cundari et al.[69]	QC(MCSCF/ECP$_S$,ECP$_S d$)	204	120.0				
	Joubert et al.[55]	QC(MP2/ECP$_D$,VDZd)	204	120.0	578	7	569	122
	Kovács[77]	QC(B3P/ECP$_D$2 fg,VTZ2df)	201.8	118.0				
		QC(B3P/ECP$_D$,VTZd)	204.6	119.2	552	15	541	135
HoF$_3$	Zasorin[56]	ED/gas (r_g)	200.7(3)	105.8(24)				
		ED/gas (r_e)	197.8(10)	108.2(32)				
	Hauge et al.[92]	IR/MI(Ne)			572.4	94	554.0	122

TABLE 1. Structural parameters [bond distances (pm) and bond angles (deg)] and vibrational frequencies (cm^{-1}) of the lanthanide trifluorides—Continued

LnF_3	Reference	Method[a]	La–X	X–La–X	ν_1	ν_2	ν_3	ν_4
		IR/MI(Ar)			556.7	104	535.6	119
		IR/MI(N_2)				124	516	143
	Dolg et al.[70]	QC(CISD+Q/$ECP_D f$,$ECP_D d$)	201.7	120.0				
	Cundari et al.[69]	QC(MCSCF/ECP_S,$ECP_S d$)	203	120.0				
	Joubert et al.[55]	QC(MP2/ECP_D,VDZd)	202	120.0	582	20	572	123
ErF_3	Bencze et al.[94]	IR/MI(Ar)			560.7		539.4	
		IR/MI(N_2)			546.0		524	
	Dolg et al.[70]	QC(CISD+Q/$ECP_D f$,$ECP_D d$)	200.4	120.0				
	Cundari et al.[69]	QC(MCSCF/ECP_S,$ECP_S d$)	202	120.0				
	Joubert et al.[55]	QC(MP2/ECP_D,VDZd)	201	120.0	585	27	576	124
	Lesar et al.[116]	QC(MP2/ECP_D,VDZ2d)	201.2	120.0	592	22	583	134
TmF_3	Bencze et al.[94]	IR/MI(Ar)			566.2		544.8	
		IR/MI(N_2)			547		529	
	Dolg et al.[70]	QC(CISD+Q/$ECP_D f$,$ECP_D d$)	199.2	120.0				
	Cundari et al.[69]	QC(MCSCF/ECP_S,$ECP_S d$)	201	120.0				
	Joubert et al.[55]	QC(MP2/ECP_D,VDZd)	200	120.0	589	35	580	124
	Lesar et al.[116]	QC(MP2/ECP_D,VDZ2d)	200.3	120.0	594	31	586	134
YbF_3	Hauge et al.[92]	IR/MI(Ne)			584.1	100	564.7	144
		IR/MI(Ar)			568.5		546.4	
		IR/MI(N_2)					526	
	Dolg et al.[70]	QC(CISD+Q/$ECP_D f$,$ECP_D d$)	197.9	120.0				
	Cundari et al.[69]	QC(MCSCF/ECP_S,$ECP_S d$)	200	120.0				
	Joubert et al.[55]	QC(MP2/ECP_D,VDZd)	199	120.0	592	39	582	125
LuF_3	Hauge et al.[92]	IR/MI(Ne)			585.4	101	570.5	150
		IR/MI(Ar)			569.6	112	552.2	144
		IR/MI(N_2)				121	530	149
	Dolg et al.[70]	QC(CISD+Q/$ECP_D f$,$ECP_D d$)	196.5	120.0				
	Cundari et al.[69]	QC(MCSCF/ECP_S,$ECP_S d$)	200	120.0				
	Lanza and Fragala[71]	QC(CAS-MCSCF/ECP_S,VDZd)	197.3	119.8	596	55	594	135
		QC(MP2/ECP_S,VDZd)	194.2	117.9	629	42	622	141
		QC(MP2/ECP_S,TZ2d)	196.2	118.7				
	Adamo and Maldivi[72]	QC(B3LYP/ECP_S,$ECP_S d$)	199.1	118.9	583	97	569	150
	Adamo and Maldivi[45]	QC(BP-DS/TZ,TZd)	196.8	117.8	580	43	571	142
		QC(B3P/ECP_S,$ECP_S d$)	198.5	118.5	589	60	573	150
		QC(BP/ECP_S,$ECP_S d$)	200.3	117.3				
	Joubert et al.[114]	QC(B3LYP/ECP_D,VDZd)	197	118.4	601	61	589	131
	Joubert et al.[55]	QC(MP2/ECP_D,VDZd)	198	120.0	597	44	588	127
	Vetere et al.[74]	QC(PBE/ECP_S,$ECP_S d$)	199.5	118.0	571	70	564	126
		QC(PBE0/ECP_S,VDZd)	196.4	118.2				
	Adamo and Barone[73]	QC(PBE0/ECP_D,$ECP_D d$)	197.7	119.3	572	40	553	141
		QC(PBE0/ECP_D,VTZd)	197.6	119.7				
		QC(PBE0/ECP_S,$ECP_S d$)	197.9	119.0	595	58	586	149
		QC(PBE0/ECP_S,VTZd)	198.3	119.0				
	Solomonik and Marochko[90]	QC(CISD+Q/$ECP_S f$,$ECP_S d$)	197.9	120.0	593	43	587	139

[a]In the basis set the first item refers to the lanthanide, whereas the second one refers to the halogen atom.

[b]ν_3 is probably perturbed from its expected location around 493 cm^{-1} by a resonance interaction with an E' electronic level resulting in an additional level around 540 cm^{-1}. The true ν_1 band is the one at 526 cm^{-1} observed in the Raman/MI(Ar) spectrum (Ref. 31).

3.2. Theoretical Studies

Theoretical investigations of LnX_3 compounds include several systematic studies dealing either with the whole lanthanide row or with selected representatives. Recent computed data obtained at adequate levels of theory are compiled in Tables 1–4. (For less sophisticated semiempirical and HF results see Meyers et al.,[58] Bender and Davidson,[59] Pyykkö and Lohr,[60] Li et al.,[61] Lohr and Jia,[62] Culberson et al.,[63] Weber et al.,[64] Ruscic et al.,[65] Ellis and Goodman,[66] DeKock et al.,[67] and DiBella et al.[68]) They can be used to analyze trends in the structural and vibrational properties of LnX_3 compounds and to assess the performance of the various theoretical levels. While the data in Tables 1–4 reflect the performance of the computational methods on a certain LnX_3 molecule, the average performance on the Ln–X bond distances along a LnX_3 row can be deduced from Table 5.

TABLE 2. Structural parameters [bond distances (pm) and bond angles (deg)] and vibrational frequencies (cm^{-1}) of the lanthanide trichlorides

$LnCl_3$	Reference	Method[a]	La–X	X–La–X	Fundamentals			
					ν_1	ν_2	ν_3	ν_4
$LaCl_3$	Zasorin[56]	ED/gas (r_g)	258.9(5)	112.8(17)				
		ED/gas (r_e)	253.8(9)	115.4(20)				
	Spiridonov et al.[24]	ED/gas (r_e)	256.0(6)	116.5(3)				
	Girichev et al.[89]	ED/gas (r_g)	258.9(6)	116.7(12)[d]				
	Selivanov et al.[25]	IR/gas					316	
	Perov et al.[26]	IR/MI(Xe)				52	300	74
	Kovács and Konings[27]	IR/gas				59	317	
		QC(MP2/ECP$_{HW}f$,VDZd)	259.7	115.7	321	35	332	70
	Dolg et al.[70]	QC(CISD+Q/ECP$_D f$,ECP$_D d$)	261.2	120.0				
	Adamo and Maldivi[72]	QC(B3LYP/ECP$_S f$,ECP$_S d$)	263.3	118.6	316[b]	43	317[b]	76
	Adamo and Maldivi[45]	QC(BP-DS/TZ,TZd)	259.0	116.5	309[b]	30	320[b]	65
		QC(B3P/ECP$_S f$,ECP$_S d$)	260.9	118.2	323[b]	45	331[b]	80
		QC(BP/ECP$_S f$,ECP$_S d$)	264.1	114.1				
	Joubert et al.[114]	QC(B3LYP/ECP$_D$,VDZd)	265	118.1	294	46	317	68
	Joubert et al.[55]	QC(MP2/ECP$_D$,VDZd)	266	120.0	289	24	313	60
	Vetere et al.[74]	QC(PBE/ECP$_S f$,ECP$_S d$)	261.8	117.0	304[b]	37	324[b]	75
		QC(PBE0/ECP$_S f$,ECP$_S d$)	260.8	118.1	312[b]	36	331[b]	75
		QC(PBE0/ECP$_S$,VDZd)	260.5	118.7				
	Adamo and Barone[73]	QC(PBE0/ECP$_D$,ECP$_D d$)	262.6	117.1	305[b]	64	325[b]	74
		QC(PBE0/ECP$_D$,VTZd)	263.0	117.5				
		QC(PBE0/ECP$_S$,ECP$_S d$)	263.3	119.0	301[b]	62	324[b]	72
		QC(PBE0/ECP$_S$,VTZd)	263.0	118.1				
	Kovács[77]	QC(B3P/ECP$_D 2 fg$,ECP$_D 2 df$)	259.6	118.0				
		QC(B3P/ECP$_D$,ECP$_D d$)	261.1	115.3	311	32	326	75
	Solomonik and Marochko[90]	QC(CISD+Q/ECP$_S 3 f$,ECP$_S d$)	259.8	120.0	314	6	332	67
$CeCl_3$	Kovács and Konings[28]	IR/gas[c]				58	321	
		QC(MP2/ECP$_D f$,VDZd)	260.2	118.8	317	20	340	71
		QC(MP2/ECP$_D$,VDZd)	264.4	120	292	26	317	61
	Cundari et al.[69]	QC(MCSCF/ECP$_S$,ECP$_S d$)	262	120.0				
	Lanza and Fragala[115]	QC(MP2/ECP$_S$,VDZd)	255.0	118.5				
		QC(MP2/ECP$_S$,TZ2d)	257.0	120.0				
		QC(MP2/ECP$_S g$,TZ2d)	255.5	118.1				
		QC(CCSD/ECP$_S$,VDZd)	255.5	119.7				
	Joubert et al.[55]	QC(MP2/ECP$_D$,VDZd)	264	120.0	291	26	316	61
$PrCl_3$	Zasorin[56]	ED/gas (r_g)	255.4(5)	112.5(15)				
		ED/gas (r_e)	251.0(9)	114.3(20)				
	Selivanov et al.[25]	IR/gas					320	
	Cundari et al.[69]	QC(MCSCF/ECP$_S$,ECP$_S d$)	261	120.0				
	Joubert et al.[55]	QC(MP2/ECP$_D$,VDZd)	262	120.0	294	27	319	62
$NdCl_3$	Selivanov et al.[25]	IR/gas					324	
	Wells et al.[91]	IR/gas			349	177	301	120
	Feltrin and Cesaro[95]	IR/MI(Ar)					328.3	
	Kovács and Konings[28]	IR/gas[c]				60	327	
		QC(MP2/ECP$_D$,VDZd)	260.3	120	298	26	324	63
	Cundari et al.[69]	QC(MCSCF/ECP$_S$,ECP$_S d$)	259	120.0				
	Joubert et al.[55]	QC(MP2/ECP$_D$,VDZd)	260	120.0	297	27	322	63
$PmCl_3$	Cundari et al.[69]	QC(MCSCF/ECP$_S$,ECP$_S d$)	258	120.0				
	Joubert et al.[55]	QC(MP2/ECP$_D$,VDZd)	259	120.0				
$SmCl_3$	Kovács and Konings[28]	IR/gas[c]				61	331	
		QC(MP2/ECP$_D$,VDZd)	257.3	120	302	31	326	66
	Cundari et al.[69]	QC(MCSCF/ECP$_S$,ECP$_S d$)	256	120.0				
	Joubert et al.[55]	QC(MP2/ECP$_D$,VDZd)	257	120.0	301	30	326	66
$EuCl_3$	Dolg et al.[70]	QC(CISD+Q/ECP$_D f$,ECP$_D d$)	252.3	120.0				
	Cundari et al.[69]	QC(MCSCF/ECP$_S$,ECP$_S d$)	255	120.0				
	Joubert et al.[55]	QC(MP2/ECP$_D$,VDZd)	255	120.0	313	32	332	70

TABLE 2. Structural parameters [bond distances (pm) and bond angles (deg)] and vibrational frequencies (cm^{-1}) of the lanthanide trichlorides—Continued

$LnCl_3$	Reference	Method[a]	La–X	X–La–X	Fundamentals ν_1	ν_2	ν_3	ν_4
$GdCl_3$	Zasorin[56]	ED/gas (r_g)	248.8(5)	112.3(12)				
		ED/gas (r_e)	244.5(7)	113.5(21)				
	Giricheva et al.[57]	ED/gas (r_g)	247.4(5)	117.0(11)[d]				
	Selivanov et al.[25]	IR/gas					326	
	Perov et al.[26]	IR/MI(Xe)				53	318	82
	Kovács and Konings[28]	IR/gas[c]				64	337	
		QC(MP2/ECP$_D$,VDZd)	254.0	120.0	305	35	328	66
	Dolg et al.[70]	QC(CISD+Q/ECP$_D f$,ECP$_D d$)	251.1	120.0				
	Cundari et al.[69]	QC(MCSCF/ECP$_S$,ECP$_S d$)	253	120.0				
	Lanza and Fragala[71]	QC(CAS-MCSCF/ECP$_S$,VDZd)	252.8	120.0	314	45	336	77
		QC(MP2/ECP$_S$,VDZd)	246.3	120.0				
		QC(MP2/ECP$_S$,TZ2d)	248.6	120.0				
	Adamo and Maldivi[72]	QC(B3LYP/ECP$_S$,ECP$_S d$)	251.8	119.0	331[b]	43	333[b]	77
	Adamo and Maldivi[45]	QC(BP-DS/TZ,TZd)	248.1	119.0	322[b]	32	337[b]	73
		QC(B3P/ECP$_S$,ECP$_S d$)	251.9	120.0	331[b]	43	333[b]	77
		QC(BP/ECP$_S$,ECP$_S d$)	251.5	120.0				
	Joubert et al.[114]	QC(B3LYP/ECP$_D$,VDZd)	253	118.8	309	43	328	72
	Joubert et al.[55]	QC(MP2/ECP$_D$,VDZd)	254	120.0	304	35	328	66
	Vetere et al.[74]	QC(PBE/ECP$_S$,ECP$_S d$)	251.0	118.6	313[b]	42	334[b]	75
		QC(PBE0/ECP$_S$,VDZd)	249.2	119.2				
	Adamo and Barone[73]	QC(PBE0/ECP$_D$,ECP$_D d$)	250.4	118.7	318[b]	36	336[b]	77
		QC(PBE0/ECP$_D$,VTZd)	250.3	118.8				
		QC(PBE0/ECP$_S$,ECP$_S d$)	249.8	119.3	318[b]	32	337[b]	74
		QC(PBE0/ECP$_S$,VTZd)	249.6	119.1				
$TbCl_3$	Zasorin[56]	ED/gas (r_g)	247.6(5)	111.2(15)				
		ED/gas (r_e)	243.8(8)	112.9(19)				
	Girichev et al.[89]	ED/gas (r_g)	247.1(5)	115.5(12)[d]				
	Cundari et al.[69]	QC(MCSCF/ECP$_S$,ECP$_S d$)	252	120.0				
	Joubert et al.[55]	QC(MP2/ECP$_D$,VDZd)	252	120.0	308	36	333	69
$DyCl_3$	Hargittai[9]	ED/gas (r_g)	246.1(8)					
	Feltrin and Cesaro[95]	IR/MI(Ar)					340.2	
	Groen[30]	IR/MI(Xe)					324.2	
		Raman/MI(Xe)			318			
	Kovács and Konings[28]	IR/gas[c]				65	340	
		QC(MP2/ECP$_D$,VDZd)	251.1	120	311	38	335	70
	Cundari et al.[69]	QC(MCSCF/ECP$_S$,ECP$_S d$)	251	120.0				
	Joubert et al.[55]	QC(MP2/ECP$_D$,VDZd)	251	120.0	310	38	334	70
	Kovács[77]	QC(B3P/ECP$_D$2 fg,ECP$_D$2df)	246.3	119.6				
		QC(B3P/ECP$_D$,ECP$_D d$)	247.5	119.2	325	28	343	84
$HoCl_3$	Zasorin[56]	ED/gas (r_g)	246.2(5)	111.7(15)				
		ED/gas (r_e)	242.5(9)	112.6(19)				
	Loktyushina et al.[97]	IR/MI(Ar)			346[e]		340	
	Cundari et al.[69]	QC(MCSCF/ECP$_S$,ECP$_S d$)	250	120.0				
	Joubert et al.[55]	QC(MP2/ECP$_D$,VDZd)	250	120.0	312	39	336	71
$ErCl_3$	Giricheva et al.[18]	ED/gas (r_g)	243.0(5)	112.3(12)				
		ED/gas (r_e)	239.3(5)					
	Perov et al.[26]	IR/MI(Xe)					328	
	Cundari et al.[69]	QC(MCSCF/ECP$_S$,ECP$_S d$)	248	120.0				
	Joubert et al.[55]	QC(MP2/ECP$_D$,VDZd)	248	120.0	314	41	338	72
$TmCl_3$	Giricheva et al.[21]	ED/gas (r_g)	242.2(6)	116.2(14)[d]				
	Feltrin and Cesaro[95]	IR/MI(Ar)					346.1	
	Cundari et al.[69]	QC(MCSCF/ECP$_S$,ECP$_S d$)	247	120.0				
	Joubert et al.[55]	QC(MP2/ECP$_D$,VDZd)	247	120.0	316	42	341	73
$YbCl_3$	Dolg et al.[70]	QC(CISD+Q/ECP$_D f$,ECP$_D d$)	243.8	120.0				
	Cundari et al.[69]	QC(MCSCF/ECP$_S$,ECP$_S d$)	247	120.0				
	Joubert et al.[55]	QC(MP2/ECP$_D$,VDZd)	246	120.0	317	43	341	73

TABLE 2. Structural parameters [bond distances (pm) and bond angles (deg)] and vibrational frequencies (cm^{-1}) of the lanthanide trichlorides—Continued

					Fundamentals			
$LnCl_3$	Reference	Method[a]	La–X	X–La–X	ν_1	ν_2	ν_3	ν_4
$LuCl_3$	Zasorin[56]	ED/gas (r_g)	241.7(6)	111.5(20)				
		ED/gas (r_e)	237.4(10)	114.5(24)				
	Giricheva et al.[19]	ED/gas (r_g)	240.3(5)	117.9(13)				
		ED/gas (r_α)	236.7(6)	120.0(15)				
	Perov et al.[26]	IR/MI(Xe)				60	331	88
	Dolg et al.[70]	QC(CISD+Q/$ECP_D f$,$ECP_D d$)	242.8	120.0				
	Cundari et al.[69]	QC(MCSCF/ECP_S,$ECP_S d$)	245	120.0				
	Lanza and Fragala[71]	QC(CAS-MCSCF/ECP_S,VDZd)	245.0	120.0	323	52	349	87
		QC(MP2/ECP_S,VDZd)	238.4	120.0	342	41	368	78
		QC(MP2/ECP_S,TZ2d)	239.7	120.0				
	Adamo and Maldivi[72]	QC(B3LYP/ECP_S,$ECP_S d$)	244.7	120.0	318[b]	75	341[b]	78
	Adamo and Maldivi[45]	QC(BP-DS/TZ,TZd)	240.0	120.0	331[b]	25	351[b]	82
		QC(B3P/ECP_S,$ECP_S d$)	242.5	120.0	323[b]	73	340[b]	77
		QC(BP/ECP_S,$ECP_S d$)	244.4	120.0				
	Joubert et al.[114]	QC(B3LYP/ECP_D,VDZd)	244	119.9	319	8	339	76
	Joubert et al.[55]	QC(MP2/ECP_D,VDZd)	246	120.0	305	60	327	80
	Vetere et al.[74]	QC(PBE/ECP_S,$ECP_S d$)	244.3	120.0	314[b]	17	338[b]	73
		QC(PBE0/ECP_S,VDZd)	242.5	120.0				
	Adamo and Barone[73]	QC(PBE0/ECP_D,$ECP_D d$)	241.9	120.0	326[b]	16	344[b]	77
		QC(PBE0/ECP_D,VTZd)	241.7	120.0				
		QC(PBE0/ECP_S,$ECP_S d$)	242.9	120.0	323[b]	25	347[b]	75
		QC(PBE0/ECP_S,VTZd)	242.4	120.0				
	Solomonik and Marochko[90]	QC(CISD+Q/$ECP_S f$,$ECP_S d$)	239.7	120.0	355	42	380	83

[a]In the basis set the first item refers to the lanthanide whereas the second one to the halogen atom.
[b]The assignment in the original papers (Refs. 45, and 72–74) is interchanged.
[c]Re-interpretation of the gas-phase spectra given by Kovács et al. (Ref. 29).
[d]Dynamic analyses of the ED results indicate planar equilibrium geometries (Refs. 57 and 89).
[e]Erroneous assignment by Loktyushina et al. (Ref. 97) of a side-band near ν_3.

All the lanthanide trihalides have been investigated by Cundari et al. at the MCSCF/ECP_S,$ECP_S d$ level,[69] except LaX_3. The complete LnF_3 and $LnCl_3$ row has been studied by Joubert et al. using the MP2/ECP_D,VDZd method.[55] Dolg et al. investigated the variation of the Ln–X bond lengths within the LnF_3 row and in selected representatives of the other halides at the configuration interaction with single and double excitations $(CISD+Q)/ECP_D f$,$ECP_D d$ level.[70] It should be noted, that the latter computations used a D_{3h} symmetry constraint for all the molecules which was justified by the very small difference in the energy (below 0.01 eV) and bond distances (below 1 pm) found between the planar and pyramidal structures. Additional systematic calculations using complete active space (CAS)-multiconfiguration self-consistent field (MCSCF), MP2, and DFT methods have been carried out for the LaX_3, GdX_3, and LuX_3 series.[45,71–74] The advantage of these molecules is that the f^0, f^7, and f^{14} electronic configurations of La^{3+}, Gd^{3+} and Lu^{3+}, respectively, lead to an $L=0$ state preventing first-order spin–orbit couplings. (The free-ion states are believed to approximate properly the electronic structure of LnX_3.) Furthermore, $J=0$ in the case of lanthanum and lutetium excluding second-order spin–orbit effects, whereas for gadolinium the second-order couplings are expected to be weak.[75]

Two works of methodological importance are noteworthy. In a series of studies Adamo et al. investigated the performance of various DFT methods, generally in conjunction with moderate basis sets.[45,72–74,76] The only exception was the BP-DS/TZ,TZd level,[45] consisting of good quality Slater-type basis functions. In their ECP studies the importance of polarization functions was noted.[74] On the other hand, their assessment of the ECP methods may be influenced by the deficiencies of the moderate basis sets used. For example, the reported good performance of the Perdew–Burke–Ernzerhof hybrid functional (PBE0)/ECP_S, valence double-zeta basis set (VDZd) level[74] can be attributed to fortunate cancellation of errors, as an extension of the halogen basis leads to corruption of the results.[73]

A recent methodological study of Kovács on $LaCl_3$ was devoted to the effect of basis set extension and the differences between the MP2 and two popular (B3LYP and B3P) DFT methods in conjunction with large basis sets.[77] The standard valence bases of La–ECP_D and Cl–ECP_D were extended gradually by polarization functions up to $(2fg)$ and $(2df)$ quality, respectively. In conjunction with DFT, the highest basis set converged satisfactorily to saturation for the molecular geometry, while the convergence was still insufficient with the MP2 method. Another deficiency of MP2 in these calculations was evident from the variation of the computed data, referring to the large sensitivity of this method on the quality of basis set. On the other hand, the basis set superposition errors (BSSE) for the $La_2Cl_6 \leftrightarrow 2\,LaCl_3$ reaction are considerable even with DFT, indicating a less satis-

TABLE 3. Structural parameters [bond distances (pm) and bond angles (deg)] and vibrational frequencies (cm^{-1}) of the lanthanide tribromides

$LnBr_3$	Reference	Method[a]	La–X	X–La–X	Fundamentals			
					ν_1	ν_2	ν_3	ν_4
$LaBr_3$	Giricheva et al.[117]	ED/gas (r_g)	274.1(5)	115.5(20)				
	Zasorin[56]	ED/gas (r_g)	274.2(4)	114.3(17)				
		ED/gas (r_e)	269.3(10)	115.0(23)				
	Kovács and Konings[27]	IR/gas				ca. 30	232	
		QC(MP2/ECP$_{HW}f$,ECP$_{HW}d$)	275.8	116.8	205	22	248	45
	Dolg et al.[70]	QC(CISD+Q/ECP$_D f$,ECP$_D d$)	277.0	120.0				
	Adamo and Maldivi[72]	QC(B3LYP/ECP$_S f$,ECP$_S d$)	277.9	118.7	245[b]	44	258[b]	80
	Adamo and Maldivi[45]	QC(BP-DS/TZ,TZd)	274.0	116.3	196[b]	26	233[b]	42
		QC(B3P/ECP$_S f$,ECP$_S d$)	275.4	118.1	208[b]	46	236[b]	66
		QC(BP/ECP$_S f$,ECP$_S d$)	277.9	114.6				
	Vetere et al.[74]	QC(PBE/ECP$_S f$,ECP$_S d$)	276.0	115.7	195[b]	25	234[b]	44
		QC(PBE0/ECP$_S f$,ECP$_S d$)	275.3	118.2	196[b]	18	242[b]	44
	Adamo and Barone[73]	QC(PBE0/ECP$_D$,ECP$_D d$)	277.1	116.3	193[b]	23	235[b]	45
		QC(PBE0/ECP$_D$,VTZd)	277.4	119.0				
		QC(PBE0/ECP$_S$,ECP$_S d$)	276.8	117.3	193[b]	19	237[b]	42
		QC(PBE0/ECP$_S$,VTZd)	277.3	118.0				
	Kovács[77]	QC(B3P/ECP$_D2 fg$,ECP$_D2 df$)	275.1	118.3				
		QC(B3P/ECP$_D$,ECP$_D d$)	276.7	115.4	195	26	234	45
	Solomonik and Marochko[90]	QC(CISD+Q/ECP$_S 3f$,ECP$_S d$)	275.6	120.0	193	13	241	43
$CeBr_3$	Cundari et al.[69]	QC(MCSCF/ECP$_S$,ECP$_S d$)	277	120.0				
	Kovács[105]	QC(MP2/ECP$_D$,ECP$_{HW}d$)	279.7	120.0	185	20	237	44
$PrBr_3$	Girichev et al.[87]	ED/gas (r_g)	269.6(6)	114.7(10)[c]				
	Cundari et al.[69]	QC(MCSCF/ECP$_S$,ECP$_S d$)	275	120.0				
$NdBr_3$	Zakharov et al.[88]	ED/gas (r_g)	267.5(6)	115.0(12)				
		ED/gas (r_e)	265.9(7)	120				
	Wells et al.[91]	IR/gas			220	120	188	80
	Cundari et al.[69]	QC(MCSCF/ECP$_S$,ECP$_S d$)	274	120.0				
$PmBr_3$	Cundari et al.[69]	QC(MCSCF/ECP$_S$,ECP$_S d$)	272	120.0				
$SmBr_3$	Cundari et al.[69]	QC(MCSCF/ECP$_S$,ECP$_S d$)	271	120.0				
$EuBr_3$	Dolg et al.[70]	QC(CISD+Q/ECP$_D f$,ECP$_D d$)	268.0	120.0				
	Cundari et al.[69]	QC(MCSCF/ECP$_S$,ECP$_S d$)	269	120.0				
$GdBr_3$	Zasorin[56]	ED/gas (r_g)	264.1(4)	113.7(20)				
		ED/gas (r_e)	259.0(9)	115.2(23)				
	Loktyushina and Mal'tsev[96]	IR/MI(Xe)					255	
		IR/MI(Ar)					238	
	Dolg et al.[70]	QC(CISD+Q/ECP$_D f$,ECP$_D d$)	266.7	120.0				
	Cundari et al.[69]	QC(MCSCF/ECP$_S$,ECP$_S d$)	268	120.0				
	Adamo and Maldivi[72]	QC(B3LYP/ECP$_S$,ECP$_S d$)	266.5	120.0	238	47	238	64
	Adamo and Maldivi[45]	QC(BP-DS/TZ,TZd)	263.0	119.8	194[b]	17	240[b]	45
		QC(B3P/ECP$_S$,ECP$_S d$)	266.2	120.0	238	47	238	64
		QC(BP/ECP$_S$,ECP$_S d$)	266.1	120.0				
	Vetere et al.[74]	QC(PBE/ECP$_S$,ECP$_S d$)	265.6	120.0	192[b]	13	239[b]	45
	Adamo and Barone[73]	QC(PBE0/ECP$_D$,ECP$_D d$)	265.2	120.0	195[b]	10	241[b]	46
		QC(PBE0/ECP$_D$,VTZd)	265.4	120.0				
		QC(PBE0/ECP$_S$,ECP$_S d$)	264.4	120.0	197[b]	19	244[b]	46
		QC(PBE0/ECP$_S$,VTZd)	264.3	120.0				
$TbBr_3$	Cundari et al.[69]	QC(MCSCF/ECP$_S$,ECP$_S d$)	267	120.0				
$DyBr_3$	Hargittai[9]	ED/gas (r_g)	260.9(8)					
	Feltrin and Cesaro[95]	IR/MI(Ar)					243.1	
	Groen[30]	IR/gas				44	243	
		IR/MI(Kr)					237.2	
		IR/MI(Xe)					229.4	
		Raman/MI(Kr)			210		237	
		Raman/MI(Xe)			202		227	47
	Cundari et al.[69]	QC(MCSCF/ECP$_S$,ECP$_S d$)	265	120.0				
	Kovács[105]	QC(MP2/ECP$_D$,ECP$_{HW}d$)	266.8	120.0	195	32	243	48

TABLE 3. Structural parameters [bond distances (pm) and bond angles (deg)] and vibrational frequencies (cm^{-1}) of the lanthanide tribromides—Continued

$LnCl_3$	Reference	Method[a]	La–X	X–La–X	Fundamentals			
					ν_1	ν_2	ν_3	ν_4
	Kovács[77]	$QC(B3P/ECP_D2\,fg,ECP_D2df\,)$	261.9	120.0				
		$QC(B3P/ECP_D,ECP_Dd)$	262.8	120.0	197	9	242	48
$HoBr_3$	Girichev et al.[87]	ED/gas (r_g)	259.5(6)	115.3(11)[c]				
	Loktyushina et al.[97]	IR/MI(Ar)			245[d]		241.5	
	Cundari et al.[69]	$QC(MCSCF/ECP_S,ECP_Sd)$	264	120.0				
$ErBr_3$	Zakharov et al.[20]	ED/gas (r_g)	258.2(6)	116.0(14)				
		ED/gas (r_e)	256.1(9)	120(2)				
	Cundari et al.[69]	$QC(MCSCF/ECP_S,ECP_Sd)$	263	120.0				
$TmBr_3$	Feltrin and Cesaro[95]	IR/MI(Ar)					249.9	
	Cundari et al.[69]	$QC(MCSCF/ECP_S,ECP_Sd)$	262	120.0				
$YbBr_3$	Dolg et al.[70]	$QC(CISD+Q/ECP_Df,ECP_Dd)$	259.4	120.0				
	Cundari et al.[69]	$QC(MCSCF/ECP_S,ECP_Sd)$	261	120.0				
$LuBr_3$	Zasorin[56]	ED/gas (r_g)	255.7(4)	115.0(11)				
		ED/gas (r_e)	251.6(8)	117.2(17)				
	Loktyushina and Mal'tsev[96]	IR/MI(Xe)					231	
		IR/MI(Ar)					245	
	Dolg et al.[70]	$QC(CISD+Q/ECP_Df,ECP_Dd)$	258.4	120.0				
	Cundari et al.[69]	$QC(MCSCF/ECP_S,ECP_Sd)$	260	120.0				
	Adamo and Maldivi[72]	$QC(B3LYP/ECP_S,ECP_Sd)$	259.0	120.0	198[b]	32	242[b]	51
	Adamo and Maldivi[45]	$QC(BP-DS/TZ,TZd)$	254.6	120.0	201[b]	20	248[b]	51
		$QC(B3P/ECP_S,ECP_Sd)$	255.2	120.0	198[b]	36	252[b]	53
		$QC(BP/ECP_S,ECP_Sd)$	257.7	120.0				
	Vetere et al.[74]	$QC(PBE/ECP_S,ECP_Sd)$	258.6	120.0	196[b]	28	242[b]	49
	Adamo and Barone[73]	$QC(PBE0/ECP_D,ECP_Dd)$	256.6	120.0	201[b]	25	245[b]	49
		$QC(PBE0/ECP_D,VTZd)$	256.7	120.0				
		$QC(PBE0/ECP_S,ECP_Sd)$	257.2	120.0	201[b]	31	247[b]	50
		$QC(PBE0/ECP_S,VTZd)$	257.2	120.0				
	Solomonik and Marochko[90]	$QC(CISD+Q/ECP_Sf,ECP_Sd)$	255.5	120.0	214	35	263	55

[a]In the basis set the first item refers to the lanthanide, whereas the second one refers to the halogen atom.
[b]The assignment in the original papers (Refs. 45 and 72–74) is interchanged.
[c]Dynamic analyses of the ED results indicate planar equilibrium geometries (Refs. 87 and 88).
[d]Erroneous assignment by Loktyushina et al. (Ref. 97) of a side-band near ν_3.

factorily convergence to saturation with regard to the energetics. Compared to the experimental geometry, the study showed the better performance of B3P and MP2 over B3LYP in conjunction with the above basis set. In general, DFT predicted a somewhat larger pyramidal character than MP2. A decreasing pyramidal character was found with increasing basis set size.

3.3. Assessment of the Ln–X Bond Distances

Recommended values for the equilibrium Ln–X bond lengths are given in Table 5. They are principally based on the comprehensive r_e data set of Zasorin.[56] It should be kept in mind, however, that in spite of the (partly) compensating dimer and anharmonicity effects these data might be affected by a small systematic error. The least affected by the errors are the fluorides, where both the dimer content[78,79] and the anharmonicity of the stretching vibrations[73] are probably negligible. In the view of the approximations used in the evaluation of the bond lengths we suggest an uncertainty of at least 2 pm for the values in Table 5.

Trends in the experimental and selected theoretical Ln–X bond distances are shown in Fig. 1. The main observations can be summarized as follows:

(i) Both the experimental and computed data demonstrate a (near) linear decreasing character of the Ln–X distances along the lanthanide row, in good agreement with the well-known "lanthanide contraction." This trend was already observed earlier and has been used to estimate yet unmeasured bond lengths.[56,80,81] The random distribution around the line is essentially within experimental errors and non-systematic errors (due to the different basis set for each element) of the computations. It should be noted that some deviations from linearity (best seen in the $LnCl_3$ series) may indicate a marginal exponential character of the decrease. For a definite conclusion, however, systematic studies with more sophisticated calculations would be required.

(ii) The computations systematically overestimate the equilibrium Ln–X bond distance, the magnitude depending on the type of halide. The average deviation of the individual theoretical levels is given in Table 6. Inspecting Table 6, the poor agreement of the estimates by Myers and Graves[7] is

TABLE 4. Structural parameters [bond distances (pm) and bond angles (deg)] and vibrational frequencies (cm^{-1}) of the lanthanide triiodides

					Fundamentals			
LnI_3	Reference	Method[a]	La–X	X–La–X	ν_1	ν_2	ν_3	ν_4
LaI_3	Hargittai[54]	ED/gas (r_α)	286(3)					
	Kovács and Konings[27]	IR/gas				25	191	
		QC(MP2/ECP$_{HW}f$,ECP$_{HW}d$)	296.8	116.0	150	19	201	33
	Dolg et al.[70]	QC(CISD+Q/ECP$_D f$,ECP$_D d$)	301.6	120.0				
	Adamo and Maldivi[72]	QC(B3LYP/ECP$_S f$,ECP$_S d$)	297.3	117.9	135[b]	32	190[b]	18
	Adamo and Maldivi[45]	QC(BP-DS/TZ,TZd)	298.3	119.4	132[b]	21	183[b]	28
		QC(B3P/ECP$_S f$,ECP$_S d$)	296.9	117.8	136[b]	26	177[b]	30
		QC(BP/ECP$_S f$,ECP$_S d$)	299.3	114.4				
	Vetere et al.[74]	QC(PBE/ECP$_S f$,ECP$_S d$)	297.5	115.4	144[b]	21	193[b]	32
		QC(PBE0/ECP$_S f$,ECP$_S d$)	296.9	118.4	142[b]	13	199[b]	31
	Adamo and Barone[73]	QC(PBE0/ECP$_D$,ECP$_D d$)	298.9	117.1	139[b]	16	192[b]	32
		QC(PBE0/ECP$_S$,ECP$_S d$)	298.1	117.0	141[b]	16	196[b]	30
	Kovács[77]	QC(B3P/ECP$_D 2 fg$,ECP$_D 2df$)	297.1	118.2				
		QC(B3P/ECP$_D$,ECP$_D d$)	298.9	115.9	142	20	192	32
	Solomonik and Marochko[90]	QC(CISD+Q/ECP$_S 3f$,ECP$_S d$)	298.1	120.0	139	14	199	32
CeI_3	Molnár et al.[17]	ED/gas (r_g)	2.948(9)					
		IR/gas				25[c]	191(10)	
	Cundari et al.[69]	QC(MCSCF/ECP$_S$,ECP$_S d$)	300	120.0				
	Kovács[105]	QC(MP2/ECP$_D$,ECP$_{HW}d$)	300.9	120.0	132	18	194	31
PrI_3	Zasorin[56]	ED/gas (r_g)	290.1(4)	113.4(13)				
		ED/gas (r_e)	285.4(7)	113.7(19)				
	Cundari et al.[69]	QC(MCSCF/ECP$_S$,ECP$_S d$)	298	120.0				
NdI_3	Zasorin[56]	ED/gas (r_g)	287.9(4)	113.8(11)				
		ED/gas (r_e)	283.5(8)	113.9(16)				
	Ezhov et al.[118]	ED/gas (r_g)	287.3(4)	118.6(11)				
		ED/gas (r_e)	286.6(5)	118(2)				
	Wells et al.[91]	IR/gas			195	98	141	72
	Cundari et al.[69]	QC(MCSCF/ECP$_S$,ECP$_S d$)	297	120.0				
PmI_3	Cundari et al.[69]	QC(MCSCF/ECP$_S$,ECP$_S d$)	295	120.0				
SmI_3	Cundari et al.[69]	QC(MCSCF/ECP$_S$,ECP$_S d$)	293	120.0				
EuI_3	Dolg et al.[70]	QC(CISD+Q/ECP$_D f$,ECP$_D d$)	291.7	120.0				
	Cundari et al.[69]	QC(MCSCF/ECP$_S$,ECP$_S d$)	292	120.0				
GdI_3	Zasorin[56]	ED/gas (r_g)	284.0(4)	115.4(13)				
		ED/gas (r_e)	279.4(7)	115.5(16)				
	Loktyushina and Mal'tsev[96]	IR/MI(Xe)					183.5	
	Dolg et al.[70]	QC(CISD+Q/ECP$_D f$,ECP$_D d$)	290.3	120.0				
	Cundari et al.[69]	QC(MCSCF/ECP$_S$,ECP$_S d$)	291	120.0				
	Adamo and Maldivi[72]	QC(B3LYP/ECP$_S$,ECP$_S d$)	288.4	120.0	138[b]	31	194[b]	35
	Adamo and Maldivi[45]	QC(BP-DS/TZ,TZd)	286.8	120.0	126[b]	19	184[b]	28
		QC(B3P/ECP$_S$,ECP$_S d$)	288.7	120.0	140[b]	30	193[b]	37
		QC(BP/ECP$_S$,ECP$_S d$)	289.3	120.0				
	Vetere et al.[74]	QC(PBE/ECP$_S$,ECP$_S d$)	287.3	120.0	138[b]	15	195[b]	33
	Adamo and Barone[73]	QC(PBE0/ECP$_D$,ECP$_D d$)	287.0	120.0	139[b]	13	196[b]	33
		QC(PBE0/ECP$_S$,ECP$_S d$)	286.1	120.0	141[b]	19	200[b]	33
TbI_3	Cundari et al.[69]	QC(MCSCF/ECP$_S$,ECP$_S d$)	289	120.0				
DyI_3	Feltrin and Cesaro[95]	IR/MI(Ar)					189.5	
	Groen[30]	IR/gas				32	195	
		IR/MI(Xe)			159		185	
		Raman/MI(Xe)			157		184	
	Cundari et al.[69]	QC(MCSCF/ECP$_S$,ECP$_S d$)	288	120.0				
	Kovács[105]	QC(MP2/ECP$_D$,ECP$_{HW}d$)	287.8	120.0	140	27	198	35
	Kovács[77]	QC(B3P/ECP$_D 2 fg$,ECP$_D 2df$)	283.5	120.0				
		QC(B3P/ECP$_D$,ECP$_D d$)	284.9	120.0	140	13	196	34

TABLE 4. Structural parameters [bond distances (pm) and bond angles in (deg)] and vibrational frequencies (cm^{-1}) of the lanthanide triiodides—Continued

LnI_3	Reference	Method[a]	La–X	X–La–X	Fundamentals			
					ν_1	ν_2	ν_3	ν_4
HoI_3	Loktyushina and Mal'tsev[96]	IR/MI(Xe)					185	
		IR/MI(Ar)					196.5	
	Cundari et al.[69]	QC(MCSCF/ECP$_S$,ECP$_S d$)	287	120.0				
ErI_3	Cundari et al.[69]	QC(MCSCF/ECP$_S$,ECP$_S d$)	286	120.0				
TmI_3	Feltrin and Cesaro[95]	IR/MI(Ar)					198.9	
	Cundari et al.[69]	QC(MCSCF/ECP$_S$,ECP$_S d$)	285	120.0				
YbI_3	Dolg et al.[70]	QC(CISD+Q/ECP$_D f$,ECP$_D d$)	282.9	120.0				
	Cundari et al.[69]	QC(MCSCF/ECP$_S$,ECP$_S d$)	283	120.0				
LuI_3	Zasorin[56]	ED/gas (r_g)	276.8(3)	115.6(6)				
		ED/gas (r_e)	273.5(6)	116.6(10)				
	Loktyushina and Mal'tsev[96]	IR/MI(Ar)					198	
	Dolg et al.[70]	QC(CISD+Q/ECP$_D f$,ECP$_D d$)	281.9	120.0				
	Cundari et al.[69]	QC(MCSCF/ECP$_S$,ECP$_S d$)	283	120.0				
	Adamo and Maldivi[72]	QC(B3LYP/ECP$_S$,ECP$_S d$)	280.9	120.0	140[b]	29	195[b]	37
	Adamo and Maldivi[45]	QC(BP-DS/TZ,TZd)	279.1	120.0	130[b]	28	184[b]	34
		QC(B3P/ECP$_S$,ECP$_S d$)	279.7	120.0	145[b]	29	195[b]	37
		QC(BP/ECP$_S$,ECP$_S d$)	280.7	120.0				
	Vetere et al.[74]	QC(PBE/ECP$_S$,ECP$_S d$)	280.4	120.0	140[b]	26	195[b]	36
	Adamo and Barone[73]	QC(PBE0/ECP$_D$,ECP$_D d$)	278.5	120.0	142[b]	23	196[b]	35
		QC(PBE0/ECP$_S$,ECP$_S d$)	279.0	120.0	144[b]	29	200[b]	37
	Solomonik and Marochko[90]	QC(CISD+Q/ECP$_S f$,ECP$_S d$)	277.2	120.0	152	32	211	40

[a]In the basis set the first item refers to the lanthanide, whereas the second one to the halogen atom.
[b]The assignment in the original papers (Refs. 45 and 72–74) is interchanged.
[c]Band not assigned by Molnár et al. (Ref. 17).

also obvious. It is not surprising, because these were based on a few early ED results and empirical considerations. Among the extensively applied computational methods the best performance was achieved at the BP–Dirac–Slater (DS)/triple-zeta basis set (TZ), TZd level.[45] Its error is 3–4 pm for the fluorides, chlorides, and bromides, whereas ~8 pm for the iodides. In fact, the BP-DS/TZ,TZd values agree very well with the r_g experimental data of the first three halides. On the other hand, the larger error of the com-

TABLE 5. Recommended Ln–X equilibrium bond distances (pm)[a]

Ln	LnF_3	$LnCl_3$	$LnBr_3$	LnI_3
La	207.7	253.4	268.9	286.7
Ce	206.8	252.2	267.6	285.7
Pr	205.8	251.1	266.4	284.8
Nd	204.9	249.9	265.2	283.8
Pm	203.9	248.8	263.9	282.9
Sm	202.9	247.6	262.7	281.9
Eu	202.0	246.5	261.5	280.9
Gd	201.0	245.3	260.3	280.0
Tb	200.1	244.2	259.0	279.0
Dy	199.1	243.0	257.8	278.1
Ho	198.1	241.9	256.6	277.1
Er	197.2	240.7	255.3	276.1
Tm	196.2	239.6	254.1	275.2
Yb	195.3	238.4	252.9	274.2
Lu	194.3	237.3	251.6	273.3

[a]Estimated uncertainty ±2 pm. The values are based on trends obtained by a joint analysis of experimental and theoretical data.

putations for the iodides is consistently shown by all the theoretical levels. Among the other DFT methods B3P/ECP$_S$,ECP$_S d$ has been selected for Fig. 1 to show their worst performance.

(iii) The magnitude of the computational error is not consistent along the lanthanide row. Generally, the deviation from experiment is the largest in the case of the LaX_3 molecules, and decreases gradually towards the LuX_3 ones. The steepest slope can be observed for the iodides.

The B3P/ECP$_D 2fg$,ECP$_D 2df$,[77] MP2/ECP$_S 3f$,ECP$_S d$, and CISD+Q/ECP$_S 3f$,ECP$_S d$[82] computational levels have been used only for a few LnX_3 compounds, yet these data suggest a performance comparable to BP-DS/TZ,TZd, cf. Tables 1–4. They reflect the previously outlined importance of the extended Gaussian valence basis sets of the present ECPs. In a recent study of $CeCl_3$, $PrCl_3$, $NdCl_3$, and $DyCl_3$ by Kapala et al.[83] a modified ECP$_D$ for the lanthanide atoms was used in conjunction with MP2 and B3LYP theories. However, their modification of the ECP$_D$ has no theoretical justification, hence the achieved excellent performance can be attributed to accidental cancellation of errors only.

3.4. Assessment of the X–Ln–X Bond Angles

While the available data could facilitate a satisfactory prediction of equilibrium Ln–X bond distances for the whole series, the experimental and theoretical X–Ln–X angles are more ambiguous. As a result of the shrinkage effect, the ef-
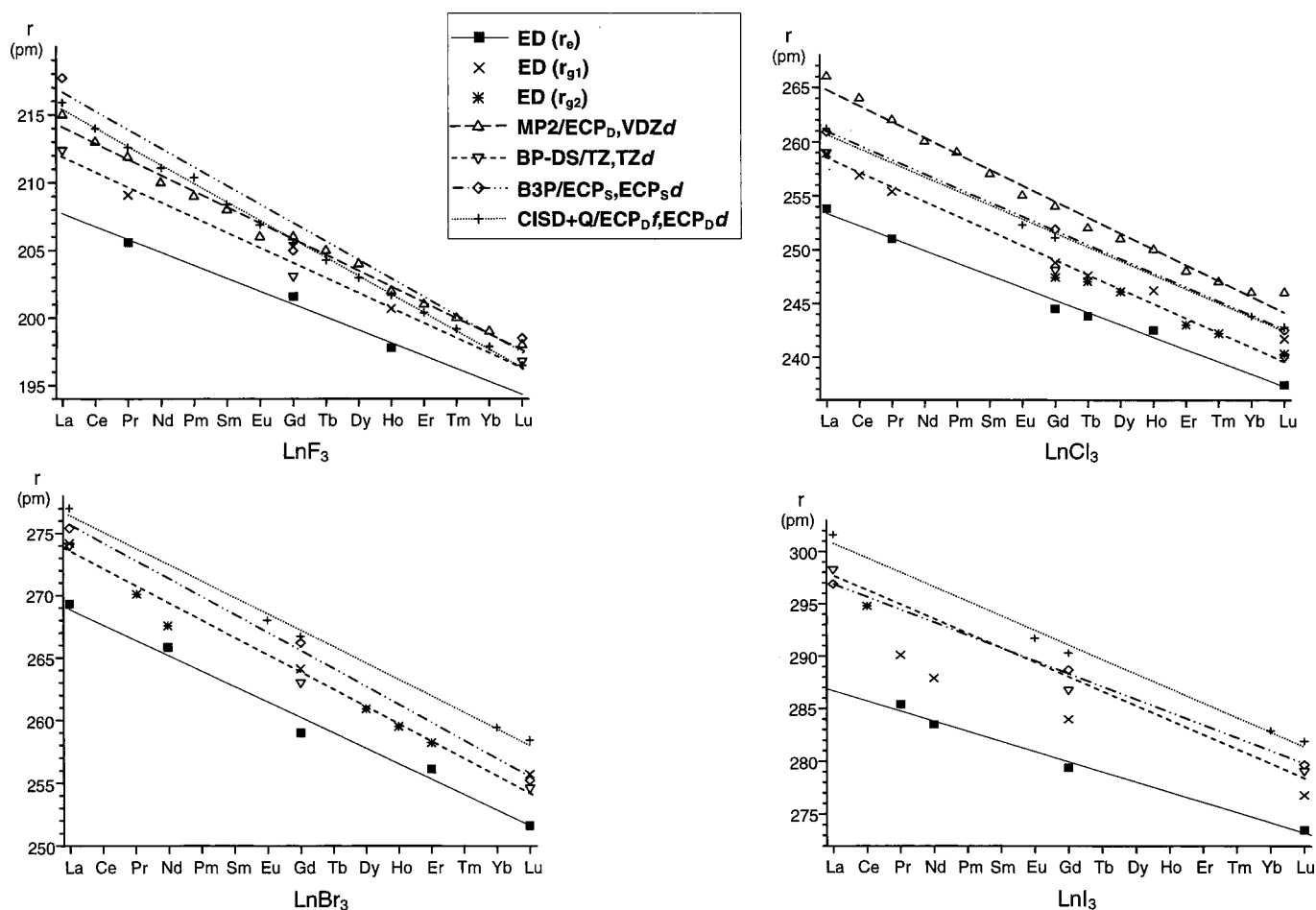
FIG. 1. Experimental and selected computed bond distances of LnX$_3$ compounds. The (r_{g1}) data represent the consistent data set of Zasorin, whereas the (r_{g2}) ones represent those from other authors.

TABLE 6. Average deviations (pm) from the recommended equilibrium Ln–X bond distances

Method[a]	LnF$_3$	LnCl$_3$	LnBr$_3$	LnI$_3$
r_g obtained by Zasorin[56]	3.4	4.2	4.4	4.2
r_g obtained by other authors[b]		3.4	3.0	
MCSCF/ECP$_S$,ECP$_S$$d$[69]	5.4	8.4	8.1	11.0
MP2/ECP$_D$,ECP$_D$$d$[55]	4.8	9.1		
MP2/ECP$_D$,VDZd[28]		9.8		
CISD+Q/ECP$_D$$f$,EC$_D$$d$[70]	4.9	6.3	7.0	11.1
BP-DS/TZ,TZd[45]	3.1	3.7	3.6	8.1
B3P/ECP$_S$,ECP$_S$$d$[45]	6.1	6.5	5.4	8.4
B3LYP/ECP$_S$,ECP$_S$$d$[72]	5.9	8.0	7.6	9.9
B3LYP/ECP$_D$,VDZd[114]	4.0	8.7		
BP/ECP$_S$,ECP$_S$$d$[45]	6.2	7.9	7.0	9.8
PBE/ECP$_S$,ECP$_S$$d$[74]	5.6	7.0	6.5	8.4
PBE0/ECP$_S$,VDZd[74]	2.7	5.4		
PBE0/ECP$_D$,ECP$_D$$d$[73]	6.0	6.3	6.1	8.1
PBE0/ECP$_D$,VTZd[73]	5.6	6.7	6.3	
PBE0/ECP$_S$,ECP$_S$$d$[73]	6.1	6.5	5.9	7.7
PBE0/ECP$_S$,VTZd[73]	5.9	5.5	6.0	
Estimations by Myers and Graves[7]	10.5	5.7	3.9	8.9

[a]In the statistics those methods were considered which have been applied at least for three compounds of an LnX$_3$ (X=F, Cl, Br, or I) row.
[b]See Tables 2 and 3.

fective bond angles obtained from ED studies are smaller than the real equilibrium values. A proper account for shrinkage would require the exact knowledge of the bending vibrations, which for low frequencies are difficult to obtain both experimentally and theoretically. In the vibrational spectra of LnX_3 compounds (especially when $X=Br$, I), these bands appear near the lower detection limit of the spectrometers and possess a broad and complex band contour. In MI spectroscopy the matrix shift is a non-negligible factor. Prediction of these low-frequency vibrations by quantum chemical computations suffers from the ambiguous potential energy surface around the minimum and the harmonic approximation used in the frequency calculations (*vide infra*). This uncertainty of the computed bending frequencies is shown in the large diversity of the data in Tables 1–4. In addition, the knowledge of the bending potential function would be very important to model the populated higher vibrational states accurately.

The shrinkage effect has been carefully analyzed in recent studies on CeI_3,[17] $GdCl_3$, $TmCl_3$, $LuCl_3$,[57] and $ErBr_3$[20] suggesting a planar (or quasiplanar) equilibrium structure for these molecules. A reanalysis of earlier electron diffraction measurements on $LaCl_3$ assuming only monomer in the gaseous phase resulted in a pyramidal equilibrium geometry with four lowest doubly degenerated vibrational levels located inside both wells of the inversion potential.[24]

Ambiguity in the bond angles is coupled with that of the shape of LnX_3 molecules. An overview of previous controversial results is given by Molnár and Hargittai.[84] The ambiguity could not be solved by quantum chemical calculations either. Even recent theoretical studies at more adequate levels showed an extreme sensitivity of the computed shape of LnX_3 compounds on the theoretical level used. Dynamic electron correlation and f functions on the lanthanide atom seem to be important for X–Ln–X angles smaller than $120°$.[77]

While the exact magnitudes of the bond angles are still dubious, the main trends in the shape of LnX_3 molecules could be established. Most of the results agree in an: (i) increasing bond angle from F to I and (ii) increasing bond angle from La to Lu. This behavior originates from the decreasing polarizability of Ln along the row[85] and the weaker polarization abilities of the heavier halogens. Polarization leads to a distortion of the electron density distribution around the metal resulting in pyramidal geometries, which is counterbalanced by increasing ligand repulsions in the heavier species favoring a planar arrangement in the latter structures.[86] A secondary effect beside the above main trends have been suggested recently by Molnár and Hargittai.[84] Their model assumes a slight impact of the $4f$ density tail on the molecular geometry and on the basis of the asphericity of the $4f$ electron shell predicts some deviations from the gradually decreasing pyramidal trend along the lanthanide row. Because of its probable small magnitude, this secondary effect may be best observed in the (most polarized) LnF_3 compounds.

Studies of the inversion barrier in pyramidal LnX_3 com-

TABLE 7. Recommended X–Ln–X equilibrium bond angles (deg)[a]

Ln	LnF_3	$LnCl_3$	$LnBr_3$	LnI_3
La	109.0	118.0	118.0	118.5
Ce	109.5	118.5	118.5	119.0
Pr	110.0	119.0	119.0	119.5
Nd	110.5	119.5	119.5	120.0
Pm	111.0	120.0	120.0	120.0
Sm	111.5	120.0	120.0	120.0
Eu	112.0	120.0	120.0	120.0
Gd	112.5	120.0	120.0	120.0
Tb	113.0	120.0	120.0	120.0
Dy	113.5	120.0	120.0	120.0
Ho	114.0	120.0	120.0	120.0
Er	114.5	120.0	120.0	120.0
Tm	115.0	120.0	120.0	120.0
Yb	115.5	120.0	120.0	120.0
Lu	116.0	120.0	120.0	120.0

[a]Estimated uncertainty: $\pm 4°$ for LnF_3; $\pm 2°$ for the other halides.

pounds resulted in values below $1\ kJ \cdot mol^{-1}$ for the chlorides, bromides and iodides.[27,73,74] In agreement with the computed smaller bond angles (*vide supra*) DFT methods predicted somewhat higher barriers (up to $3.2\ kJ \cdot mol^{-1}$ in LaF_3)[73] than *ab initio* calculations.[68,70] Nevertheless, the low barriers of the heavier species can be close or below the ground state level of the inversion vibration, referring to an effectively planar (in spectroscopic terms quasiplanar) molecular geometry. An accurate prediction of the potential energy surface of LnX_3 compounds would require highly sophisticated calculations with complete electron correlation treatment and saturated basis set.

Our recommendations for the equilibrium bond angles of LnX_3 compounds (compiled in Table 7) are derived from the available experimental and theoretical information. On the basis of the relatively small experimental and computed bond angles of the trifluorides and of the ν_1 bands found in the IR/MI spectra, probably all the LnF_3 compounds are pyramidal. Because of the rough account for the shrinkage effect by Zasorin,[56] bond angles somewhat larger than his experimental ones are suggested here. The absence of the ν_1 bands in the IR spectra, the ED results on $PrBr_3$,[87] $NdBr_3$,[88] and CeI_3[17] and the computed very small inversion barriers for $LnCl_3$, $LnBr_3$, and LnI_3[27] imply a quasiplanar character for the trichlorides, tribromides, and triiodides of the light lanthanides. We note the very close bond angles of $LaCl_3$, $LaBr_3$, and LaI_3,[27,77] indicating a similar shape of the three halides (cf. Tables 2–4). On the basis of recent experimental[17,18,20,57,89] and theoretical results,[45,73,77,90] the trichlorides, tribromides, and triiodides of the heavier lanthanides should be planar.

4. Vibrational Frequencies

4.1. Experimental Data

The normal modes of LnX_3 molecules are represented by

$$\Gamma_{C_{3v}} = 2A_1 + 2E$$

and

$$\Gamma_{D_{3h}} = A_1' + A_2'' + 2E'$$

for pyramidal and planar structures, respectively. According to the selection rules, the A_1/A_2'' and the degenerate E/E' modes can appear in both the IR and Raman spectra, whereas the symmetric stretch, ν_1 (A_1'), of planar structures is forbidden in the IR. Moreover, the computations indicate very low IR intensity for ν_1 in pyramidal, and for the asymmetric bend ν_4 (E/E') in both structures.[27,28,77]

Experimental data on the molecular vibrations of lanthanide trihalides are limited and rather discordant. Early gas-phase IR data on the asymmetric stretching fundamentals are available for $LaCl_3$, $PrCl_3$, $NdCl_3$, and $GdCl_3$.[25] Recently, new gas-phase FT-IR measurements have been performed on several trichlorides and on the LaX_3 and DyX_3 ($X=Cl,Br,I$) molecules.[27,28,30] In these new measurements two of the four fundamentals, the asymmetric stretching, ν_3 (E/E'), and symmetric bending, ν_2 (A_1/A_2''), have been detected. The new FT-IR ν_3 frequencies are in good agreement with the previous results for $LaCl_3$ and $NdCl_3$,[25] while there is a deviation of 11 cm^{-1} for $GdCl_3$. On the other hand, the interpretation of early gas-phase IR measurements of Wells *et al.* on NdX_3 ($X=Cl,Br,I$) compounds[91] were obviously in error, because their spectra disagree with both those of Selivanov *et al.*[25] and Kovács *et al.*[28]

In addition to the above gas-phase IR studies numerous IR/MI[26,67,92–97] and a few Raman/MI measurements[30,31] have been made on LnX_3 compounds. Because of the extremely high evaporation temperatures of the LnF_3 species their vibrational data could be obtained only under matrix-isolated conditions.[67,92,93]

4.2. Theoretical Data

The vibrational frequencies have been computed in most theoretical studies discussed in the previous section. The advantage of computations is that they can give all the four fundamentals of LnX_3 molecules. However, in contrast to the case of the r_e molecular geometries, the experimental and reported theoretical frequencies have a different physical meaning. Computation of vibrational frequencies in the routine way is based on the harmonic approximation, whereas the molecular vibrations are anharmonic. The anharmonicity may alter the harmonic frequencies up to 10–20 cm^{-1} in such molecules. This calls for caution in the interpretation of an eventual good match of experimental and computed frequencies: it does not necessarily indicate a good performance of the computation, but could be a fortunate cancellation of errors of the theoretical level used. Nevertheless, beside the scarce experimental information the computed data can be very useful in the evaluation of trends for most vibrations.

We must recall here the link between the computed molecular geometry and vibrations. Errors in the computed geometry are reflected in the potential energy surface, thus in the computed vibrational frequencies as well. An overestimation of the bond distance means underestimated bond strength, hence underestimated frequencies. In certain cases,

this error can compensate well for the neglect of anharmonicity in the computations. Considerable uncertainty originates from the errors in the computed bond angles and thus in the bending potential curves. The inversion (ν_2) mode calls for special attention. In the case of pyramidal structures with a small barrier inside of the double-minimum potential curve the computation of this mode using the harmonic model is completely irrelevant. In the above way this frequency is obtained by fitting a quadratic function (parabola) to the bottom part of the potential curve, whereas the vibrational levels are determined by the whole double-minimum potential. The harmonic approximation can only be applied satisfactorily for planar or pyramidal structures with high inversion barriers.

The complete set of experimental and computed vibrational frequencies is compiled in Tables 1–4. The experimental and selected computed results are depicted in Figs. 2–5. We note the interchanged assignment of ν_1 and ν_3 for the $LnCl_3$, $LnBr_3$, and LnI_3 series in Refs. 45, and 72–74 following erroneously the estimated frequencies of Myers and Graves.[7] Based on the reported computed IR intensities by Adamo and Barone[73] a corrected assignments is given in our tables and figures. rms deviations of the computed frequencies from the gas-phase values averaged over the lanthanide row are compiled in Table 8.

4.3. Fundamental Frequencies of LnCl$_3$ Compounds

The largest number of experimental gas-phase data has been reported for the $LnCl_3$ compounds. Additionally, these compounds have been a popular target for both MI spectroscopic and theoretical studies, hence they are the best suited to assess the matrix effects and the performance of the computations. Therefore we discuss first the $LnCl_3$ results and the data of the other halides will be analyzed in subsequent subsections, taking into account the observations made for the $LnCl_3$ series.

Figure 2 demonstrates a general linearly increasing trend of the four fundamental frequencies along the lanthanide row. Both trends originate from the "lanthanide contraction": a decrease of the bond length along the lanthanide row (cf. Fig. 1) is consistent with stronger bonds, hence larger stretching force constants. At the same time, the forces against bending become also larger with the halogens getting closer to each other. The small scattering around the experimental trendlines may be partly ascribed to the ambiguity of locating the band origin in the broad and complex gas-phase bands and to accidental matrix shifts. Some computed results deviate from the gradually increasing trend: these are the B3P/ECP$_S$,ECP$_S$d frequencies for ν_1, ν_2, and ν_4, the BP-DS/TZ,TZd frequencies for ν_2, and the salient MP2/ECP$_D$,VDZd results for $EuCl_3$ and $LuCl_3$. The deviations for ν_2 are the clear consequence of the ambiguity of the computed inversion potential curve and the deficiency of the harmonic model for these floppy molecules (*vide supra*).
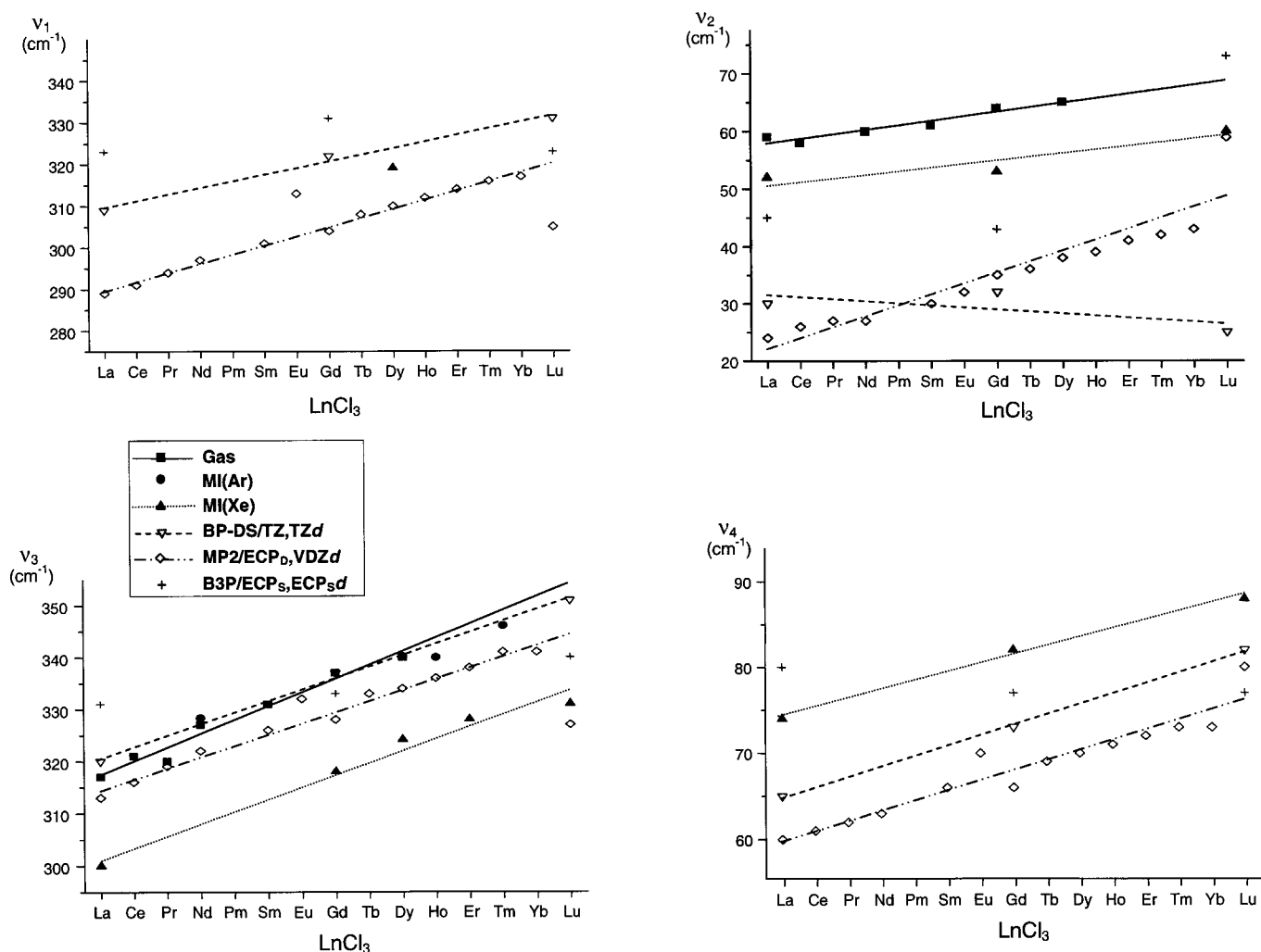
FIG. 2. Experimental and selected computed vibrational frequencies of $LnCl_3$ compounds.

Noteworthy is the very bad performance of the $B3P/ECP_S,ECP_Sd$ level, predicting erroneous slopes or scattering frequencies along the lanthanide row in many cases (see also the other halides). That such large random errors can appear even at adequate levels, suggests that caution must be taken interpreting results from computations using an untested theoretical level.

Due to the (conveniently) high frequency and large IR intensity of the ν_3 mode, the experimental information is most extensive for this fundamental. Table 2 and Fig. 2 reveal a nearly perfect agreement between the gas-phase ν_3 frequencies and those obtained in the Ar matrix. The shift in the Xe matrix is $-17\ cm^{-1}$.

A considerable number of gas-phase IR frequencies is also available for the ν_2 fundamentals. They are extended by a few IR/MI(Xe) data with a matrix shift of $-7\ cm^{-1}$. Due to the small values of these frequencies the slope of the trendlines is near horizontal. This means that the ν_2 frequencies can accurately be predicted along the lanthanide row even on the basis of a single experimental value. The inad-

equacy of computations for this fundamental (cf. Fig. 2) make the experimental information crucial.

For the ν_1 fundamentals of $LnCl_3$ compounds only a single reliable experimental value, that from the Raman/MI(Xe) measurement of $DyCl_3$,[30] is available. Although the gas-phase IR spectra of some $LnCl_3$ compounds were first interpreted in terms of overlapping ν_1 and ν_3 bands,[29] subsequent reinvestigations confirmed the complex band structure of ν_3 and rejected an unambiguous assignment of the close-lying (and weak or not IR active) ν_1 mode.[27,28]

Because of their very small IR activity also the ν_4 fundamentals are difficult to determine in the gas-phase spectra.[27,28] In fact, this fundamental has been detected only in the IR/MI(Xe) measurements on $LaCl_3$, $GdCl_3$, and $LuCl_3$.[26]

The linear trend along the lanthanide row found for the fundamentals facilitates the estimation of the missing vibrational frequencies of $LnCl_3$ compounds. Based on the compiled results we can make more accurate predictions than suggested previously.[7,98] The data in Table 9 have been
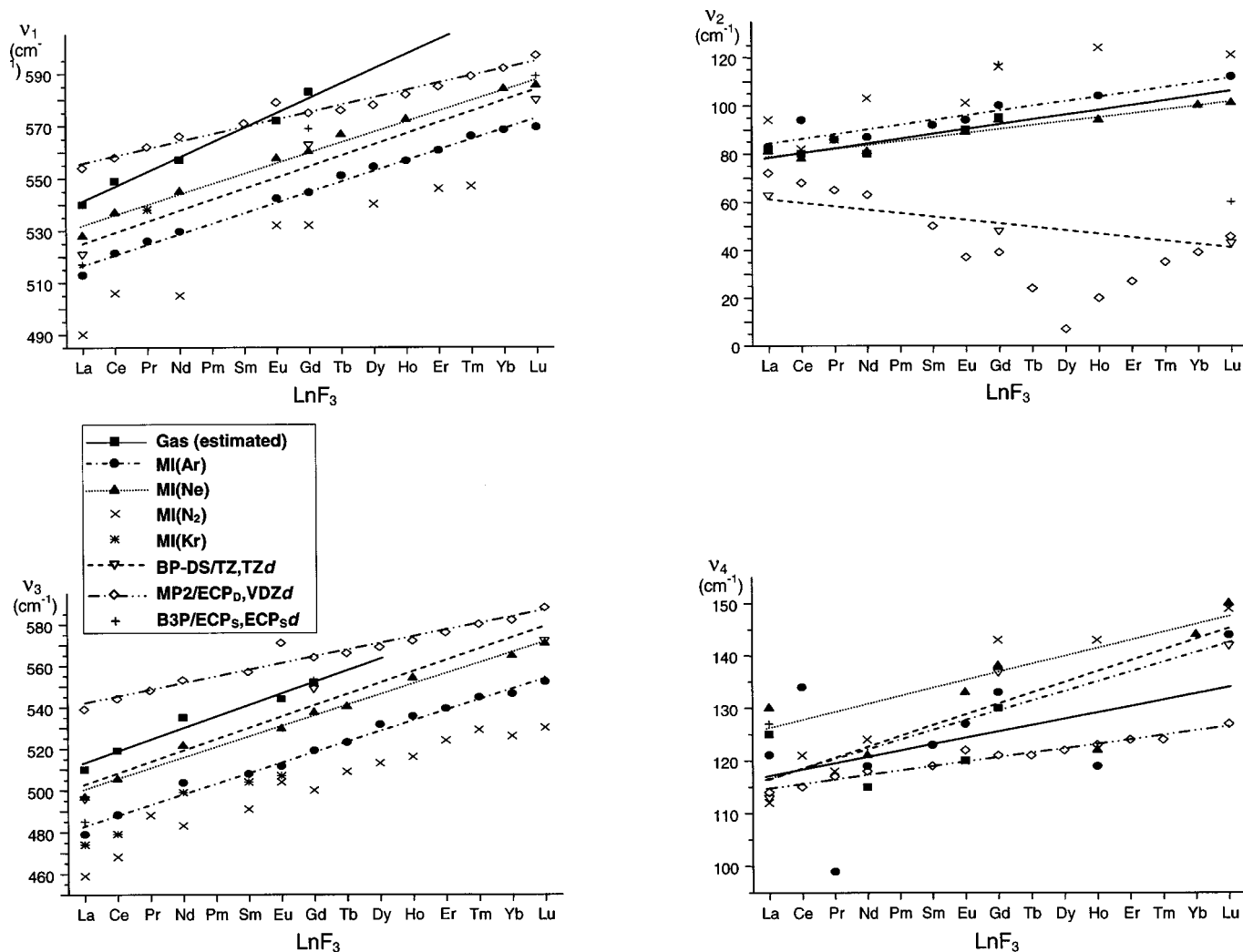
FIG. 3. Experimental and selected computed vibrational frequencies of LnF$_3$ compounds.

evaluated using the following considerations:

(1) ν_1: Estimation of the "gas-phase" frequencies was based on the single experimental Raman/MI(Xe) value of DyCl$_3$ assuming a similar matrix shift of -17 cm^{-1} found for ν_3, and a slope lower by $\sim 20\%$ than that of ν_3 (as found in the LnF$_3$ MI/IR data, *vide infra*). On that basis the assignment of the ν_1 of HoCl$_3$ (and similarly that of HoBr$_3$, *vide infra*) to a side-band of ν_3 in the IR/MI(Ar) spectrum by Loktyushina *et al.*[97] is not justified.

(2) ν_2: The frequencies of species for which no measurements have been made have been estimated solely on the basis of the available gas-phase experimental data.

(3) ν_3: Based on the excellent agreement between the gas-phase and MI(Ar) frequencies the relationship for estimation of the unmeasured ν_3 values was evaluated from the merged data set.

(4) ν_4: The "gas-phase" frequencies were estimated on the basis of the MI(Xe) data assuming a similar matrix shift of -7 cm^{-1} like found for ν_2.

An assessment of the computational methods (Table 8) reveals the superiority of the BP-DS/TZ,TZd[45] level for estimation of the vibrational frequencies of LnCl$_3$ compounds parallel to that found for the bond distances (*vide supra*). It gave an excellent agreement for the ν_3 fundamentals, and the closest (although somewhat underestimated) values for ν_1 and ν_4. The agreement of the MP2/ECP$_D$,ECP$_D d$ level was found to be somewhat worse. Except for ν_2, both methods show systematic errors for the molecular vibrations. In practical sense this means that they can be more easily corrected than most DFT calculations, that gave scattering values in several cases. An additional noteworthy feature is that the error of the calculations, even at the best levels, is not consistent for the two stretching frequencies ν_1 and ν_3. The reason may lie in the different anharmonicity and coupling patterns of the two vibrations. The excellent performance of the calculations of Kapala *et al.*[83] for CeCl$_3$, PrCl$_3$, NdCl$_3$, and DyCl$_3$ is due again to the accidental cancellation of errors using the modified ECP$_D$ (*vide supra*).
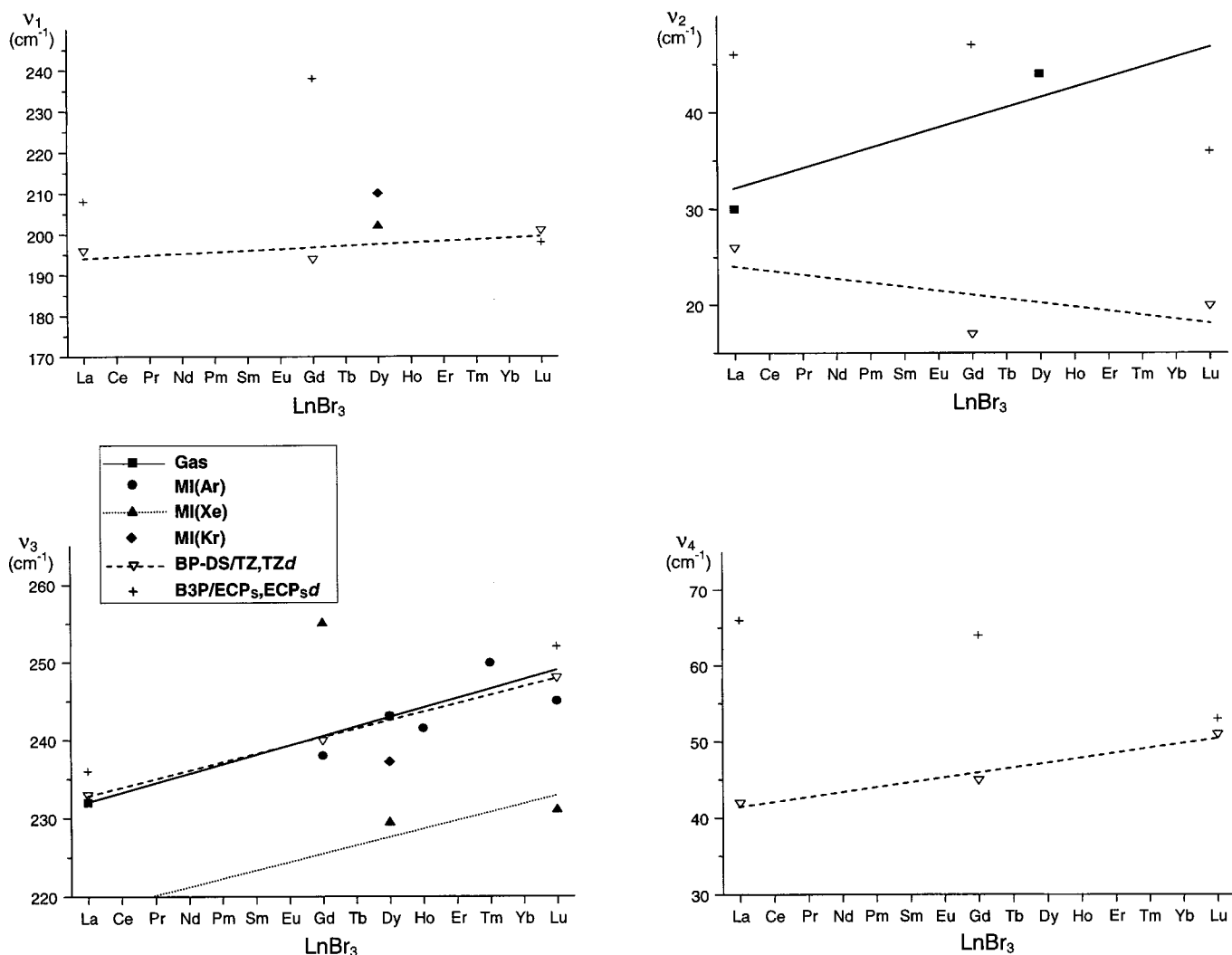
FIG. 4. Experimental and selected computed vibrational frequencies of LnBr$_3$ compounds.

4.4. Fundamental Frequencies of LnF$_3$ Compounds

Due to the extremely high evaporation temperatures required for the fluorides, gas-phase vibrational spectra have not been reported for LnF$_3$ compounds. Hastie et al.[92,93] and Wesley and DeKock[99] performed IR/MI studies of LaF$_3$, CeF$_3$, PrF$_3$, NdF$_3$, SmF$_3$, EuF$_3$, GdF$_3$, TbF$_3$, HoF$_3$, YbF$_3$, and LuF$_3$ using Ne, Ar, Kr, and N$_2$ matrices. The results on LaF$_3$, CeF$_3$, NdF$_3$, and EuF$_3$ from the two sources show a good agreement (cf. Table 1). In most cases all the four fundamentals could be identified in the spectra. The assignment of the symmetric stretching (ν_1) bands in the IR/MI spectra[92] (questioned by Wesley and DeKock[99]) was confirmed by a Raman/MI(Ar) measurement of PrF$_3$ by Lesiecki et al.[31] Recently, IR/MI experiments have been performed on DyF$_3$, ErF$_3$, and TmF$_3$ by Bencze et al.[94] reporting the stretching frequencies obtained in Ar and N$_2$ matrices.

The "gas-phase" frequencies (ν_g) of some LnF$_3$ species have been estimated by Hastie et al.[93] The stretching frequencies have been evaluated using Eq. (1),[100] where ν_{Ne}

and ν_{Ar} are the frequencies measured in the Ne and Ar matrix, respectively. For the "gas-phase" bending frequencies the mean of the two MI values was suggested.

$$\nu_g \approx \nu_{Ne} + (0.8 \pm 0.4)(\nu_{Ne} - \nu_{Ar}). \qquad (1)$$

The experimental vibrational data of LnF$_3$ compounds depicted in Fig. 3 indicate a linear trend with a marginal random scattering for the two stretching fundamentals. In agreement with the stronger matrix effects of N$_2$, the deviations are somewhat larger in these data series. A linearly increasing trend along the lanthanide row can be observed for the bending frequencies as well. Their larger scattering around the trendline can be understood by the floppy nature of these molecules, which enables a deformation of the bond angles (consequently the bending potential function) already upon weak matrix forces.

The theoretical data show similar characteristics to those discussed at the LnCl$_3$ compounds. The peculiar variation of the MP2/ECP$_D$,ECP$_D d$ ν_2 frequencies deserves a special note, because it demonstrates clearly the deficiency of the
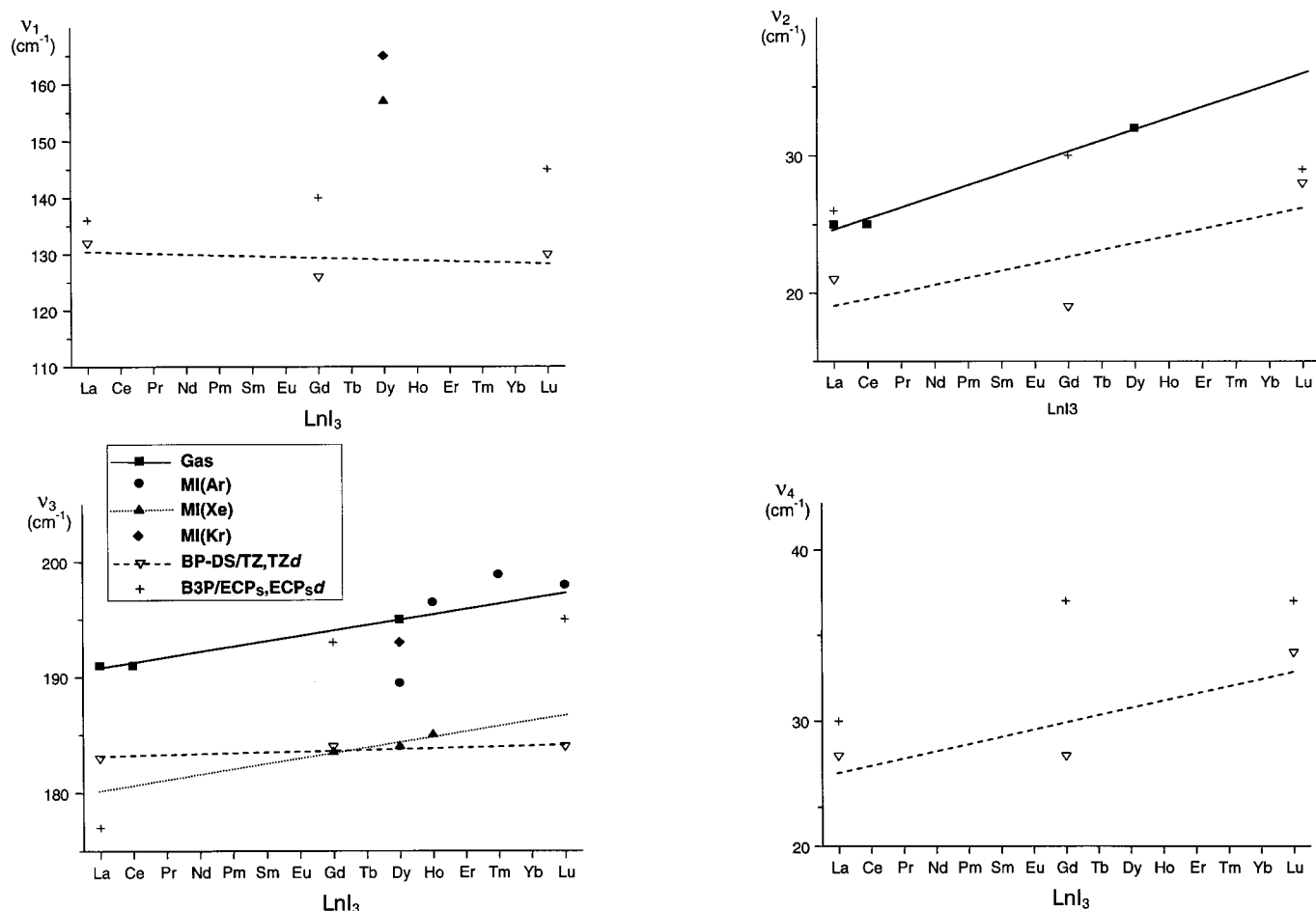
FIG. 5. Experimental and selected computed vibrational frequencies of LnI_3 compounds.

harmonic model in calculation of the inversion frequencies for double-minimum systems with a small inversion barrier. The MP2 computed bond angles increase from LaF_3 till $120°$ in the planar DyF_3 accompanied by a parallel decrease of the computed barrier. Accordingly, the flatness of the potential curve around the sub-minimum increase towards DyF_3. Hence, the harmonic model potential fitted to the subminimum results in gradually decreasing frequencies. In the computed planar structures from DyF_3 to LuF_3 the above error is not present anymore, because the inversion potential starts to resemble more and more to a quadratic (parabola) curve. In this range the computed frequencies return to the experimental trend.

Our estimated ''gas-phase'' frequencies are compiled in Table 10. They are primarily based on the MI data taking into account the following considerations:

(i) ν_1, ν_3: To our opinion, the ''gas-phase'' stretching frequencies by Hastie et al. are somewhat overestimated. A general validity of Eq. (1)[100] can be questioned on the basis of the extensive collection of vibrational data on various metal halides in Ref. 9 and the observed excellent agreement between the gas-phase and MI(Ar) frequencies of the $LnCl_3$ compounds (vide supra). Our recommended ''gas-phase'' stretching frequencies are supported by the BP-DS/TZ,TZd

computations: the overestimation of the Ln–F bond by this level is similar to that of the Ln–Cl bonds (cf. Table 6), thus a similar systematic error for the LnF_3 and $LnCl_3$ stretching frequencies can also be expected. This condition fits to the MI(Ne) experimental data, serving thus as basis for our estimated ''gas-phase'' stretching frequencies in Table 10.

ν_2, ν_4: In agreement with Hastie et al.,[93] we suggest the mean of the MI(Ne) and MI(Ar) values for the ''gas-phase'' frequencies of LnF_3 bending fundamentals.

4.5. Fundamental Frequencies of $LnBr_3$ and LnI_3 Compounds

As demonstrated in Tables 3,4 and Figs. 4,5, there are very scarce experimental and even computational data for $LnBr_3$ and LnI_3 compounds. The experimental data include the gas-phase IR measurements of $LaBr_3$, $DyBr_3$, LaI_3, CeI_3, and DyI_3 reporting ν_2 and ν_3.[17,27,30] The large uncertainty of the experimental ν_2 frequency is due to the fact that this fundamental appears near the lower limit of the IR detectors, hence its band shape could not be accurately analyzed. Additionally, a few IR/MI and Raman/MI data are available for the stretching fundamentals of the Dy, Ho, Tm and Lu trihalides.[30,95–97] The very good agreement between the gas-

TABLE 8. rms deviations of the computed frequencies from the recommended "gas-phase" values (cm^{-1})

	Method[a]	ν_1	ν_2	ν_3	ν_4
LnF_3	Myers and Graves[7]	(+)12.6	(+)4.8	(+)14.6	(−)7.3
	$MP2/ECP_D,ECP_D d$[55]	(+)15.2	(−)49.5	(+)27.8	(−)14.4
	$BP-DS/TZ,TZd$[45]	(−)8.0	(−)43.7	7.9	(−)6.7
	$B3P/ECP_S,ECP_S d$[45]	10.0	29.0	13.3	3.5
	$B3LYP/ECP_S,ECP_S d$[72]	6.6	16.5	11.8	(+)5.3
	$B3LYP/ECP_D,VDZd$[114]	(+)18.8	31.3	(+)28.8	(−)11.2
	$PBE/ECP_S,ECP_S d$[74]	10.3	(−)23.7	10.6	12.0
	$PBE0/ECP_D,ECP_D d$[73]	9.7	41.4	16.3	4.1
	$PBE0/ECP_S,ECP_S d$[73]	(+)10.6	(−)33.4	(+)19.3	(+)5.3
$LnCl_3$	Myers and Graves[7]	9.3	(−)7.4	(−)11.5	(−)4.8
	$MP2/ECP_D,ECP_D d$[55]	(−)26.5	(−)27.8	(−)6.2	(−)19.9
	$BP-DS/TZ,TZd$[45]	(−)10.7	(−)35.0	(+)1.8	(−)14.7
	$B3P/ECP_S,ECP_S d$[45]	12.8	14.2	10.1	(−)12.2
	$B3LYP/ECP_S,ECP_S d$[72]	15.3	15.0	(−)6.1	(−)12.0
	$B3LYP/ECP_D,VDZd$[114]	(−)23.9	(−)37.6	(−)8.2	(−)16.2
	$PBE/ECP_S,ECP_S d$[74]	(−)22.0	(−)34.5	8.5	(−)15.2
	$PBE0/ECP_D,ECP_D d$[73]	(−)15.1	34.5	6.0	(−)12.8
	$PBE0/ECP_S,ECP_S d$[73]	(−)17.5	31.2	4.5	(−)15.0
$LnBr_3$	Myers and Graves[7]	(+)53.8	(+)6.1	(+)16.9	(+)6.3
	$BP-DS/TZ,TZd$[45]	(−)17.5	(−)18.1	(−)0.9	(−)14.0
	$B3P/ECP_S,ECP_S d$[45]	19.2	8.5	3.2	8.5
	$B3LYP/ECP_S,ECP_S d$[72]	29.1	8.8	15.6	15.5
	$PBE/ECP_S,ECP_S d$[74]	(−)20.4	(−)17.4	4.3	(−)14.0
	$PBE0/ECP_D,ECP_D d$[73]	(−)17.9	(−)20.0	2.9	(−)13.4
	$PBE0/ECP_S,ECP_S d$[73]	(−)17.2	(−)15.7	3.7	(−)14.0
LnI_3	Myers and Graves[7]	(+)22.8	(+)2.5	(−)13.3	(+)4.1
	$BP-DS/TZ,TZd$[45]	(−)36.6	(−)6.7	(−)11.4	(−)12.5
	$B3P/ECP_S,ECP_S d$[45]	(−)25.4	(−)1.2	(−)8.2	(−)8.0
	$B3LYP/ECP_S,ECP_S d$[72]	(−)28.0	(+)3.2	(−)2.2	(−)14.2
	$PBE/ECP_S,ECP_S d$[74]	(−)25.4	(−)8.9	2.5	(−)8.7
	$PBE0/ECP_D,ECP_D d$[73]	(−)25.7	(−)11.8	1.9	(−)9.1
	$PBE0/ECP_S,ECP_S d$[73]	(−)23.7	(−)8.5	(+)4.4	(−)9.1

[a]In the statistics those methods were considered, which have been applied at least for three compounds of an LnX_3 (X=F, Cl, Br, or I) row. Consistent over- and underestimations are indicated by (+) and (−), respectively.

TABLE 9. Experimental (italics) and recommended "gas-phase" frequencies (cm^{-1}) of $LnCl_3$ compounds[a]

Ln	$\nu_1(A_1)$	$\nu_2(A_1)$	$\nu_3(E)$	$\nu_4(E)$
La	318	*59*[b]	*317*[b]	84
Ce	320	*58*[c]	*321*[c]	85
Pr	322	60	*320*[d]	86
Nd	324	*60*[c]	*327*[c]	87
Pm	326	61	328	88
Sm	327	*61*[c]	*331*[c]	89
Eu	329	63	332	90
Gd	331	*64*[c]	*337*[c]	91
Tb	333	64	337	92
Dy	335	*65*[c]	*340*[c]	93
Ho	337	66	342	94
Er	339	66	344	95
Tm	341	67	347	96
Yb	343	68	349	97
Lu	345	69	351	98

[a]Estimated error for both the experimental and estimated data is ± 10 cm^{-1}.
[b]Measured by Kovács and Konings.[27]
[c]Measured by Kovács and Konings.[28]
[d]Measured by Selivanov *et al.*[25]

phase and MI(Ar) frequencies found for the ν_3 fundamental of the $LnCl_3$ series can also be observed in the case of the $LnBr_3$ and LnI_3 compounds. Likewise, the computed BP-DS/TZ,TZd ν_3 frequencies agree well with gas-phase experimental data for the bromides, whereas they are underestimated by ~ 10 cm^{-1} in the case of the iodides. The latter error is in agreement with the considerably overestimated Ln–I bond distances by that theoretical level, as compared to $LnCl_3$ and $LnBr_3$ (cf. Fig. 1).

The estimated ν_2 and ν_3 "gas-phase" frequencies of the $LnBr_3$ and LnI_3 halides given in Tables 11 and 12, respectively, were evaluated on the basis of the gas-phase and MI(Ar) values. The single MI(Xe) and MI(Kr) experimental data of $DyBr_3$ and the MI(Xe) ones of DyI_3 were used to estimate the "gas-phase" ν_1 frequencies of the whole series, assuming a similar matrix-shift as observed for ν_3. We note the erroneous assignment of the ν_1 of $HoBr_3$ to a higher frequency side band at ν_3 in the IR/MI(Ar) spectrum by Loktyushina *et al.*[97]

The estimated ν_4 frequencies have no experimental support. Based on the observations in the LnF_3 and $LnCl_3$ series, the slope of the gradual increase along the lanthanide row was estimated on a gradually decreasing basis from F to I

TABLE 10. Recommended "gas-phase" frequencies (cm^{-1}) of LnF$_3$ compounds[a]

Ln	$\nu_1(A_1)$	$\nu_2(A_1)$	$\nu_3(E)$	$\nu_4(E)$
La	532	79	501	123
Ce	536	81	506	125
Pr	540	83	511	127
Nd	544	85	516	128
Pm	548	86	521	130
Sm	552	88	526	132
Eu	556	90	531	133
Gd	560	91	536	135
Tb	564	93	541	137
Dy	568	95	546	138
Ho	572	96	551	140
Er	576	98	556	142
Tm	580	100	561	143
Yb	584	101	566	145
Lu	588	103	572	147

[a]Estimated uncertainty ± 10 cm^{-1}.

(for the same fundamental), from ν_3 to ν_1, and from ν_4 to ν_2 (for an LnX$_3$ compound).

5. Structural and Vibrational Properties of the Ln$_2$X$_6$ Dimers

The formation of Ln$_2$Cl$_6$ dimers in the vapors of LaCl$_3$, EuCl$_3$ and LuCl$_3$ has been indicated early by Hastie *et al.*[101] Dimer formation of lanthanide trihalides in the gaseous phase has been confirmed in numerous subsequent studies. The amount of dimers was mostly estimated by the relative peak intensities in the MS spectrum,[15,16,78,79,102–104] and in a few cases by joint ED/MS analysis.[18–21] The available results are in agreement with a few percent of dimer in the vapors of the lighter lanthanide trichlorides, tribromides and triiodides, which can increase up to $\sim 20\%$ in the heavier

TABLE 11. Experimental (italics) and recommended "gas-phase" frequencies (cm^{-1}) of LnBr$_3$ compounds[a]

Ln	$\nu_1(A_1)$	$\nu_2(A_1/A_2)$	$\nu_3(E)$	$\nu_4(E)$
La	207	*30*[b]	*232*[b]	57
Ce	208	36	233	57
Pr	209	36	234	58
Nd	210	37	236	58
Pm	211	37	237	59
Sm	212	37	238	59
Eu	213	38	239	60
Gd	214	38	241	60
Tb	215	39	242	61
Dy	216	*44*[c]	*243*[c]	61
Ho	217	39	244	62
Er	218	40	245	62
Tm	219	40	247	63
Yb	220	41	248	63
Lu	221	41	249	64

[a]Estimated error for the experimental ν_3 values is ± 5 cm^{-1}, while for the experimental ν_2 and estimated frequencies ± 10 cm^{-1}.
[b]Measured by Kovács and Konings.[27]
[c]Measured by Groen.[30]

TABLE 12. Experimental (italics) and recommended "gas-phase" frequencies (cm^{-1}) of LnI$_3$ compounds[a]

Ln	$\nu_1(A_1)$	$\nu_2(A_1/A_2)$	$\nu_3(E)$	$\nu_4(E)$
La	162	*25*[b]	*191*[b]	40
Ce	163	27	*191*[c]	41
Pr	163	28	192	41
Nd	164	28	192	41
Pm	164	28	193	42
Sm	165	28	194	42
Eu	165	28	194	42
Gd	166	29	195	42
Tb	166	29	195	43
Dy	167	*32*[d]	*195*[d]	43
Ho	167	29	196	43
Er	168	29	197	44
Tm	168	30	198	44
Yb	168	30	198	44
Lu	169	30	199	45

[a]Estimated error for the experimental ν_3 values is ± 5 cm^{-1}, while for the experimental ν_2 and estimated frequencies ± 10 cm^{-1}.
[b]Measured by Kovács and Konings.[27]
[c]Measured by Molnár *et al.*[17]
[d]Measured by Groen.[30]

lanthanide analogues.[9,104] The increased stability of the dimers of heavier lanthanides is supported by the computed dissociation energies.[77] For the fluorides experimental data are available only for La$_2$F$_6$ and Ce$_2$F$_6$.[78,79] They show a negligible ($10^{-2}\%$) amount of dimers in the vapor. This small amount is seemingly in conflict with the computed highest dissociation energies for the fluoride dimers with respect to the chloride, bromide and iodide ones.[77] However, the computations referred to 0 K and did not include the entropy contribution, which is extremely important at high temperatures. Both the larger masses and smaller vibrational frequencies of the heavier halides lead to a higher entropy value.

A few dimer structures (Fig. 6) have been reported in ED[9,17–20] and theoretical studies (Table 13).[77,83,105] In most ED investigations some parameters were assumed to be equal with those of the monomers whereas others were treated independently in the refinements.[17–20] However, the small relative abundance of the dimers in the vapor and the strong correlation between the monomer and dimer structural parameters claim for aid from quantum chemical calculations in order to obtain reliable data.[9] High-level theoretical calcu-
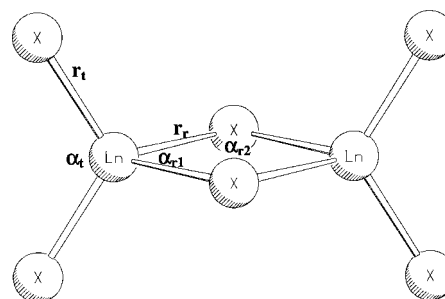

FIG. 6. The structure of Ln$_2$X$_6$ dimers.

TABLE 13. Experimental and computed geometrical parameters of Ln_2X_6 dimers

Reference	Ln_2X_6	Geometry[a]				
		r_r	r_t	α_{r1}	α_{r2}	α_t
Kovács[77]	La_2F_6[b]	236.2	212.6	70.6	109.4	116.7
Kovács[77]	Dy_2F_6[b]	221.9	200.8	73.0	107.0	117.2
Kovács[77]	La_2Cl_6[b]	281.4	258.4	80.6	99.4	117.0
Hargittai[9]	Dy_2Cl_6[d]	268.0(10)	244.9(10)	84.1(34)		
Kovács[77]	Dy_2Cl_6[b]	266.4	245.2	83.6	96.4	116.7
Giricheva et al.[18]	Er_2Cl_6[d]	265(4)	244.4(5)	84(10)		117(5)
Giricheva et al.[19]	Lu_2Cl_6[e]	258.9(24)	236.6(5)	84(2)		119(7)
Kovács[77]	La_2Br_6[b]	297.1	273.9	83.7	96.3	115.0
Kovács[105]	Ce_2Br_6[f]	301.3	278.1	83.9	96.1	117.0
Hargittai[9]	Dy_2Br_6[d]	281.1(9)	259.4(8)	91.7(17)		
Kovács[77]	Dy_2Br_6[b]	282.0	260.4	87.0	93.0	115.7
Zakharov et al.[20]	Er_2Br_6[d]	275.8(20)	258.8(6)	81(7)		116(7)
Kovács[77]	La_2I_6[b]	318.8	296.1	87.6	92.4	114.5
Molnár et al.[17]	Ce_2I_6[d]	320.7(23.8)	294.8(9)			
Kovács[105]	Ce_2I_6[f]	322.0	299.3	88.5	91.5	116.7
Kovács[77]	Dy_2I_6[b]	303.6	282.4	90.8	89.2	115.3

[a] r_r, α_{r1}, and α_{r2} indicate the geometrical parameters of the ring, while r_t and α_t the terminal ones of the dimer (cf Fig. 6).
[b] Computed at the $B3P/ECP_D2\,fg$, $VTZ2df$(Ln_2F_6), and $B3P/ECP_D2\,fg$, ECP_D2df (other dimers) level.
[c] Computed at the $B3LYP/ECP_Df$, $VDZd$ level.
[d] r_g parameters from gas-phase ED.
[e] r_α parameters from gas-phase ED.
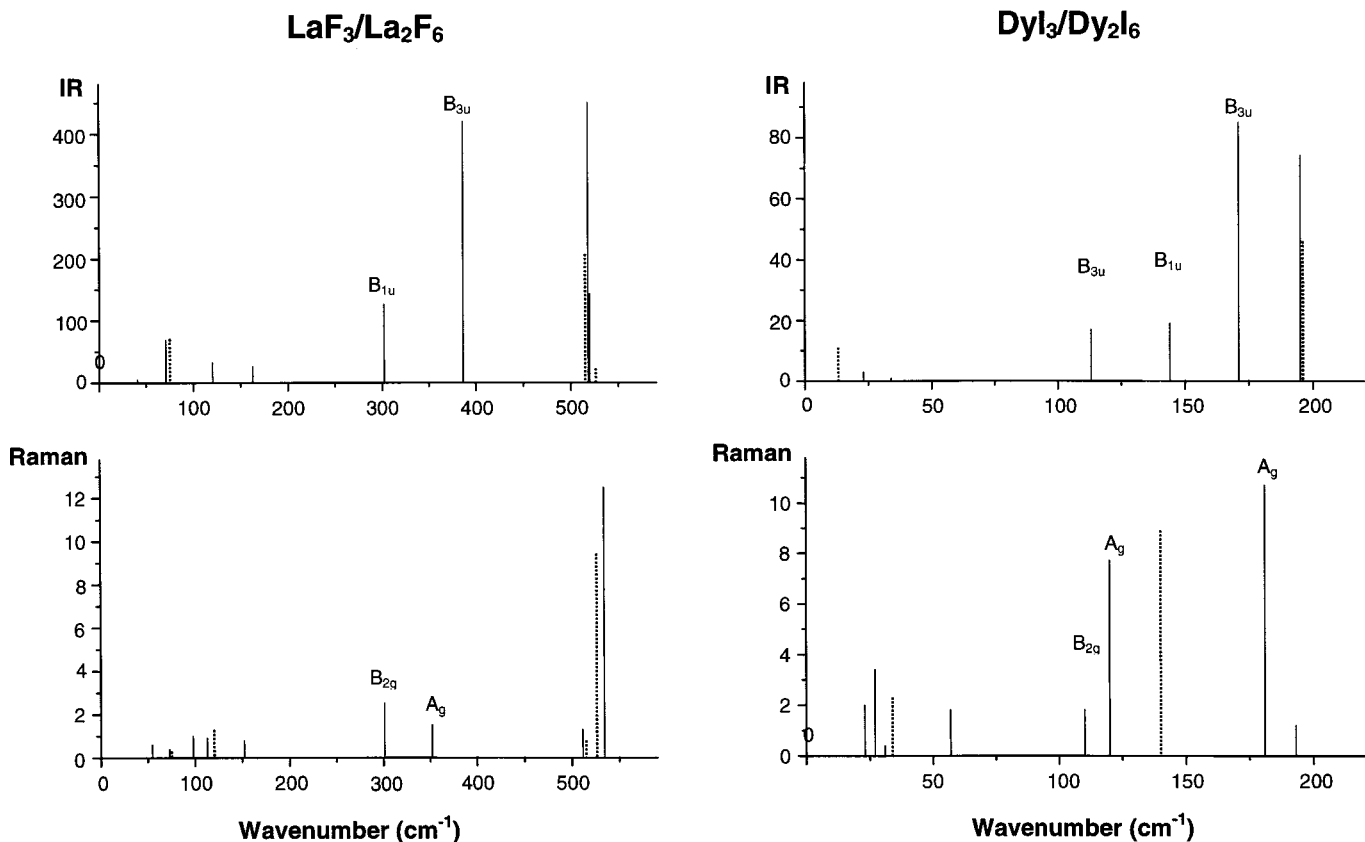[f] Computed at the $MP2/ECP_D$, $ECP_{HW}d$ level.

FIG. 7. Comparison of the IR and Raman spectra of LaF_3 and DyI_3 (dotted lines) with those of their dimers (solid lines) from $B3P/ECP_Df$, ECP_Dd computations.

TABLE 14. Comparison of experimental and computed IR frequencies[a] (cm^{-1}) of selected Ln_2X_6 compounds

Ln_2X_6	Reference	Method	Fundamentals		
			B_{1u}	B_{2u}	B_{3u}
La_2F_6	Kovács[77]	QC(B3P/ECP$_D f$, VTZd)	302 (126)	518 (450)	520 (143)
			71 (69)	163 (26)	386 (420)
				41 (5)	120 (32)
	Hastie et al.[93]	IR/MI(Ne)	313	505	520
				166	372
		IR/MI(Ar)	304	490	507
					364
		IR/MI(N$_2$)	299	468	484
					370
Dy_2Br_6	Kovács[77]	QC(B3P/ECP$_D f$,ECP$_D d$)	173 (28)	243 (104)	220 (96)
			29 (8)	55 (1)	154 (46)
				8 (<1)	47 (2)
	Feltrin and Cesaro[95]	IR/MI(Ar)			215.7
Dy_2I_6	Kovács[77]	QC(B3P/ECP$_D f$,ECP$_D d$)	144 (19)	195 (74)	171 (85)
			23 (3)	39 (<1)	113 (17)
				5 (<1)	34 (1)
	Feltrin and Cesaro[95]	IR/MI(Ar)			171.6

[a]Computed IR intensities (km/mol) are given in parentheses. There are no experimental data for fundamentals belonging to the A_u (1) and to the only Raman active A_g (4), B_{1g} (2), B_{2g} (2), and B_{3g} (1) species.

lations indicate shorter terminal Ln–X bonds (by ~1 pm) and longer ring Ln–X bonds (by ~20 pm) in the dimers with respect to the bond in the monomers.[77] The above mentioned ED studies[17–20] could not reproduce the shorter character of the terminal bonds whereas recent results from Hargittai reflect properly this feature (cf. Table 13).[9]

Except a few and mostly tentative assignments in IR/MI spectra experimental information on the molecular vibrations of the dimers is not available. On the other hand, the full vibrational spectrum has been computed for the La_2X_6 and Dy_2X_6 (X=F to I) series[77] and for Ce_2Br_6 and Ce_2I_6.[105] Representative computed IR and Raman spectra of selected LnX_3/Ln_2X_6 pairs are depicted in Fig. 7. The computations confirmed the observed five fundamentals of La_2F_6 by Hastie et al.[93] as well as the reported single bands of Dy_2Br_6 and Dy_2I_6 by Feltrin and Cesaro.[95] Based on the computed frequencies and IR intensities we revised the assignments of Hastie et al.[93] in Table 14. Keeping in mind the matrix shifts, a good agreement between the experimental and computed spectra is evident. However, the low frequency computed fundamentals should be treated with caution, because they may have a similar error as those of the monomers.

Comparison of the data in Table 14 with those of the monomers (Table 1–4) shows that the computations reproduce the relative positions of the monomer and dimer IR bands very well. This supports that computations are well suited to predict the differences between the properties of monomers and dimers of such compounds, assumed already in the ED studies of Dy_2Cl_6 and Dy_2Br_6 utilizing geometrical constraints from computations.[9] Lacking sufficient data we feel that an estimation of the geometrical and vibrational parameters for the whole Ln_2X_6 series is not justified at this moment.

6. Conclusions

In the present paper a critical review of experimental and theoretical data on the structure and molecular vibrations of lanthanide trihalides has been presented. The recent results from experimental and computational studies, which are of improved quality, confirmed previously suggested trends in the molecular properties of the title compounds and facilitated the estimation of the unmeasured values in the series. On the basis of the collected data a comparative analysis of the experimental and computational results has been performed. From present standard computational techniques the BP–DS/TZ,TZd method, incorporated in the Amsterdam Density Functional package, gave the best performance for LnX_3 compounds implying the superiority of Slater type basis functions and the direct treatment of relativistic effects. For the levels using ECPs the importance of the extended valence basis set should be emphasized.

On the basis of the joint experimental and theoretical information we evaluated a set of equilibrium geometrical parameters (Tables 5 and 7) of the title molecules. We emphasize, however, that they should be considered together with the given errors. In the view of the approximations used in the electron diffraction technique the uncertainty is at least 2 pm for the bond distances and 4° (LnF_3) or 2° (other halides) for the bond angles. Recommended values for the fundamental frequencies of the title compounds have been compiled in Tables 9–12. Because they are based on gas-phase or MI (corrected for matrix shift) experiments they are undoubtedly superior over the empirical ones of Myers and Graves[7] which are generally used as reference up to now. With the present recommended data set an old request of lanthanide physical chemistry for reliable structural and vibrational

properties is satisfied. As a first application, they have been used in the (re)-evaluation of the enthalpies of formation of gaseous lanthanide trihalides.[106]

From the assessment of the available structural and vibrational data we can conclude that still considerable efforts are needed in order to determine the molecular properties of the title compounds with an accuracy comparable to those of organic molecules of similar size. This requires the extension of experimental studies on a larger scale of compounds, a careful analysis of the possible errors and the effects of approximations in the experimental methods as well as routine application of advanced auxiliary techniques for interpretation of the experimental information. For the latter a crucial role can be foreseen for the theoretical methods provided their performance will be improved considerably.

Nevertheless, our comparative analysis showed already several advantages of the computations. Taking into account their systematic errors, the Ln–X bond distances can be predicted with sufficient accuracy. The same systematic errors appear in the computation of the dimers facilitating the determination of their structures, in which the experimental methods alone are less superior due to the small dimer fraction in the vapor. The connection of the errors between the geometry and molecular vibrations can be used as secondary information in structural and vibrational studies. On the other hand, considerable improvement is still required in the computation of bond angles and bending vibrations. Today's revolutionary hardware development opens the way for sophisticated theoretical levels, which can describe the floppy systems of most LnX_3 molecules more accurately than present routine methods.

7. Acknowledgments

8. Appendix: Abbreviations and Symbols

BP	Becke–Perdew86 exchange-correlation functional[52,111]
B3LYP	Becke3–Lee–Yang–Parr exchange-correlation functional[50,51]
B3P	Becke3–Perdew86 exchange-correlation functional[50,52]
CAS-MCSCF	complete active space multiconfiguration SCF method[107]
CCSD(T)	coupled cluster with all single and double excitations including additionally triple excitations noniteratively[110]
CISD+Q	configuration interaction with all single and double excitations including correction for size-consistency errors[109]
DFT	density functional theory
DS	relativistic Dirac–Slater calculation
d, f, g	polarization functions
ECP_D	quasirelativistic effective core potential of Dolg *et al.*[35,36]
ECP_{HW}	relativistic effective core potential of Hay and Wadt[43]
ECP_S	relativistic effective core potential of Stevens *et al.*[37,42]
ED	electron diffraction
IR	infrared spectroscopy
MCSCF	multiconfiguration SCF method[108]
MI	matrix isolation
MP2	second order Møller-Plesset perturbation
PBE	Perdew–Burke–Ernzerhof functional[112,113]
PBE0	HF/Perdew–Burke–Ernzerhof hybrid functional[76]
QC	quantum chemical computation theory[47]
Raman	Raman spectroscopy
r_e	equilibrium bond distance
r_g	thermal average distance corresponding to the temperature of the ED experiment
r_α	distance between average nuclear positions at a given temperature
TZ	triple-zeta basis set
VDZ	valence double-zeta basis set
VTZ	valence triple-zeta basis set
ν_1	symmetric stretch
ν_2	symmetric bend (inversion)
ν_3	asymmetric stretch
ν_4	asymmetric bend

9. References

[1] G. N. Lewis, M. Randall, K. S. Pitzer, and L. Brewer, *Thermodynamics* (McGraw–Hill, New York, 1961).

[2] *NIST-JANAF Thermochemical Tables*, 4th ed., *J. Phys. Chem. Ref. Data, Monograph No. 9*, edited by M. W. Chase, Jr. (1998).

[3] S. A. Cotton, *Lanthanides and Actinides* (MacMillan, London, 1991).

[4] N. Kaltsoyannis and P. Scott, *The f Elements* (Oxford University Press, Oxford, 1999).

[5] L. Cecille, M. Casarci, and L. Pietrelli, *New Separation Chemistry Techniques for Radioactive Waste and Other Specific Applications* (Commission of the European Communities, Elsevier, London, 1991).

[6] K. Hilpert and U. Niemann, Thermochim. Acta **299**, 49 (1997).

[7] C. E. Myers and D. T. Graves, J. Chem. Eng. Data **22**, 436 (1977).

[8] *Landolt-Börnstein: Numerical Data and Functional Relationships in Science and Technology*, New Series, Group II: Molecules and Radicals, Structure Data of Free Polyatomic Molecules, Subvolume A, Inorganic Molecules, Vol. 25, edited by K. Kuchitsu (Springer, Heidelberg, 1998).

[9] M. Hargittai, Chem. Rev. **100**, 2233 (2000).

[10] M. H. Brooker and G. N. Papatheodorou, in *Advances in Molten Salt Chemistry*, edited by G. Mamanton (Elsevier, Amsterdam, 1983), Vol. 5.

[11] S. Boghosian and G. N. Papatheodorou, in *Handbook on the Physics and Chemistry of Rare Earths*, edited by K. A. Geschneider, Jr. and L. Eyring (Elsevier, Amsterdam, 1996), Vol. 23, p. 435.

[12] E. Z. Zasorin, A. A. Ivanov, L. I. Ermolaeva, and V. P. Spiridonov, Russ. J. Phys. Chem. **63**, 363 (1989).

[13] S. J. Cyvin, *Molecular Vibrations and Mean Square Amplitudes* (Universitatsforlaget, Oslo, Norway, 1968).

[14] V. A. Sipachev, J. Mol. Struct. (Theochem) **121**, 143 (1985).

[15] O. Kaposi, L. Lelik, and K. Balthazar, High Temp. Sci. **16**, 299 (1983).

[16] O. Kaposi, Z. Ajtony, A. Popovic, and J. Marsel, J. Less-Common Met. **123**, 199 (1986).

[17] J. Molnár, R. J. M. Konings, M. Kolonits, and M. Hargittai, J. Mol. Struct. **375**, 223 (1996).

[18] N. I. Giricheva, G. V. Girichev, S. A. Shlykov, and O. V. Pelipets, J. Struct. Chem. (Engl. Transl.) **41**, 231 (2000).

[19] N. I. Giricheva, G. V. Girichev, A. V. Krasnov, and O. G. Krasnova, J. Struct. Chem. (Engl. Transl.) **41**, 388 (2000).

[20] A. V. Zakharov, N. I. Giricheva, N. Vogt, S. A. Shlykov, J. Vogt, and G. V. Girichev, J. Chem. Soc., Dalton Trans. 3160 (2001).

[21] N. I. Giricheva, G. V. Girichev, and A. V. Krasnov, J. Struct. Chem. (Engl. Transl.) **41**, 149 (2000).

[22] V. P. Spiridonov, A. G. Gershikov, E. Z. Zasorin, and B. S. Butayev, in *Diffraction Studies on Non-Crystalline Substances*, edited by I. Hargittai and W. J. Orville-Thomas (Elsevier, Amsterdam, 1981), p. 159.

[23] A. G. Gershikov and V. P. Spiridonov, Zh. Strukt. Khim. **27**, 30 (1986).

[24] V. P. Spiridonov, A. G. Gershikov, and V. S. Lyutsarev, J. Mol. Struct. **221**, 79 (1990).

[25] G. K. Selivanov, N. S. Yu, and A. A. Mal'tsev, Russ. J. Phys. Chem. **47**, 1239 (1973).

[26] P. A. Perov, S. V. Nedyak, and A. A. Mat'tsev, Vestn. Mosk. Univ. Khim **30**, 281 (1975).

[27] A. Kovács and R. J. M. Konings, Chem. Phys. Lett. **268**, 207 (1997).

[28] A. Kovács and R. J. M. Konings, Vibr. Spectrosc. **15**, 131 (1997).

[29] A. Kovács, R. J. M. Konings, and A. S. Booij, Vibr. Spectrosc. **10**, 65 (1995).

[30] P. C. Groen (unpublished).

[31] M. Lesiecki, J. W. Nibler, and C. W. DeKock, J. Chem. Phys. **57**, 1352 (1972).

[32] I. R. Beattie, P. J. Jones, and N. A. Young, Chem. Phys. Lett. **177**, 579 (1991).

[33] M. Dolg, in *Encyclopedia of Computational Chemistry*, edited by P. v. R. Schleyer, N. L. Allinger, T. Clark, J. Gasteiger, P. A. Kollman, H. F. Schaefer III, and P. R. Schreiner (Wiley, Chichester, 1998), p. 1478.

[34] M. Dolg and H. Stoll, in *Handbook on the Physics and Chemistry of Rare Earths*, edited by K. A. Geschneider Jr. and L. Eyring (Elsevier, Amsterdam, 1996), Vol. 22, Chap. 152.

[35] M. Dolg, H. Stoll, A. Savin, and H. Preuss, Theor. Chim. Acta **75**, 173 (1989).

[36] M. Dolg, H. Stoll, and H. Preuss, Theor. Chim. Acta **85**, 441 (1993).

[37] T. R. Cundari and W. J. Stevens, J. Chem. Phys. **98**, 5555 (1993).

[38] M. Dolg, Ph. D. thesis, University of Stuttgart, 1989.

[39] X. Cao and M. Dolg, J. Chem. Phys. **115**, 7348 (2001).

[40] X. Cao and M. Dolg, J. Mol. Struct. (Theochem) **581**, 139 (2002).

[41] http://www.theochem.uni-stuttgart.de/

[42] W. J. Stevens, M. Krauss, H. Basch, and P. G. Jasien, Can. J. Chem. **70**, 612 (1992).

[43] P. J. Hay and W. R. Wadt, J. Chem. Phys. **82**, 299 (1985).

[44] F. M. Bickelhaupt and E. J. Baerends, Rev. Comput. Chem. **15**, 1 (2000).

[45] C. Adamo and P. Maldivi, J. Phys. Chem. A **102**, 6812 (1998).

[46] T. Ziegler, V. Tschinke, E. J. Baerends, J. G. Snijders, and W. Ravenek, J. Phys. Chem. **93**, 3050 (1989).

[47] C. Møller and M. S. Plesset, Phys. Rev. **46**, 618 (1934).

[48] *Recent Developments and Applications of Modern Density Functional Theory*, edited by J. M. Seminario (Elsevier, Amsterdam, 1996).

[49] T. Veszprémi and M. Fehér, *Quantum Chemistry. Fundamentals to Applications* (Kluwer, New York, 1999), Chap. 12.

[50] A. D. Becke, J. Chem. Phys. **98**, 5648 (1993).

[51] C. Lee, W. Yang, and R. G. Parr, Phys. Rev. B **37**, 785 (1988).

[52] J. P. Perdew, Phys. Rev. B **33**, 8822 (1986).

[53] G. Frenking and N. Fröhlich, Chem. Rev. **100**, 714 (2000).

[54] M. Hargittai, J. Phys. Chem. A **103**, 7552 (1999).

[55] L. Joubert, G. Picard, and J. J. Legendre, Inorg. Chem. **37**, 1984 (1998).

[56] E. Z. Zasorin, Russ. J. Phys. Chem. (Engl. Transl.) **62**, 441 (1988).

[57] N. I. Giricheva, A. V. Zakharov, S. A. Shlykov, and G. V. Girichev, J. Chem. Soc., Dalton Trans., 3401 (2000).

[58] C. E. Meyers, L. J. Norman, and L. M. Loew, Inorg. Chem. **17**, 21 (1978).

[59] C. F. Bender and E. R. Davidson, J. Inorg. Nucl. Chem. **42**, 721 (1980).

[60] P. Pyykkö and L. L. Lohr, Inorg. Chem. **20**, 1950 (1981).

[61] L.-M. Li, J.-Q. Ren, G.-X. Xu, K. H. Hsu, and X.-Z. Wang, Int. J. Quantum Chem. **23**, 1305 (1983).

[62] L. L. Lohr and Y. Q. Jia, Inorg. Chim. Acta **119**, 99 (1986).

[63] J. C. Culberson, P. Knappe, N. Rösch, and M. C. Zerner, Theor. Chim. Acta **71**, 21 (1987).

[64] J. Weber, H. Berthou, and C. K. Jorgensen, Chem. Phys. **26**, 69 (1977).

[65] B. Ruscic, G. L. Goodman, and J. Berkowitz, J. Chem. Phys. **78**, 5443 (1983).

[66] D. E. Ellis and G. L. Goodman, Int. J. Quantum Chem. **25**, 185 (1984).

[67] R. L. DeKock, M. A. Peterson, L. K. Timmer, E. J. Baerends, and P. Vernooijs, Polyhedron **9**, 1919 (1990).

[68] S. DiBella, G. Lanza, and I. L. Fragala, Chem. Phys. Lett. **214**, 598 (1993).

[69] T. R. Cundari, S. O. Sommerer, L. A. Strohecker, and L. Tippett, J. Chem. Phys. **103**, 7058 (1995).

[70] M. Dolg, H. Stoll, and H. Preuss, J. Mol. Struct. (Theochem) **235**, 67 (1991).

[71] G. Lanza and I. L. Fragala, Chem. Phys. Lett. **255**, 341 (1996).

[72] C. Adamo and P. Maldivi, Chem. Phys. Lett. **268**, 61 (1997).

[73] C. Adamo and V. Barone, J. Comput. Chem. **21**, 1153 (2000).

[74] V. Vetere, C. Adamo, and P. Maldivi, Chem. Phys. Lett. **325**, 99 (2000).

[75] O. Kahn, *Molecular Magnetism* (VCH, New York, 1993), Chap. 3.

[76] C. Adamo and V. Barone, J. Chem. Phys. **110**, 6158 (1999).

[77] A. Kovács, Chem. Phys. Lett. **319**, 238 (2000).

[78] J. A. Roberts Jr. and A. W. Searcy, High Temp. Sci. **4**, 411 (1972).

[79] H. B. Skinner and A. W. Searcy, J. Phys. Chem. **75**, 108 (1971).

[80] A. V. Krasnov, N. I. Giricheva, and G. V. Girichev, Zh. Strukt. Khim. **17**, 667 (1976).

[81] M. Hargittai, Coord. Chem. Rev. **91**, 35 (1988).

[82] V. G. Solomonik and O. Y. Marochko, J. Struct. Chem. (Engl. Transl.) **41**, 725 (2000).

[83] J. Kapala, S. Roszak, S. N. Cesaro, and M. Miller, J. Alloys Compd. **345**, 90 (2002).

[84] J. Molnár and M. Hargittai, J. Phys. Chem. **99**, 10780 (1995).

[85] K. M. S. Saxena and S. Fraga, J. Chem. Phys. **57**, 1800 (1972).

[86] L. Joubert, B. Silvi, and G. Picard, Theor. Chem. Acc. **104**, 109 (2000).

[87] G. V. Girichev, N. I. Giricheva, S. A. Shlykov, A. V. Zakharov, A. V. Krasnov, and O. G. Krasnova, XIX. Austin Symposium on Molecular Structure, Austin, Texas, 2002.

[88] A. V. Zakharov, N. Vogt, S. A. Shlykov, N. I. Giricheva, J. Vogt, and G. V. Girichev, Struct. Chem. **14**, 193 (2003).

[89] G. V. Girichev (unpublished).

[90] V. G. Solomonik and O. Y. Marochko, Russ. J. Phys. Chem. (Engl. Transl.) **74**, 2094 (2000).

[91] J. C. Wells Jr., J. B. Gruber, and M. Lewis, Chem. Phys. **24**, 391 (1977).

[92] R. H. Hauge, J. W. Hastie, and J. L. Margrave, J. Less-Common Met. **23**, 359 (1971).

[93] J. W. Hastie, R. H. Hauge, and J. L. Margrave, J. Less-Common Met. **39**, 309 (1975).

[94] L. Bencze, A. Feltrin, S. N. Cesaro, and A. Popovic, Rapid Commun. Mass Spectrom. **10**, 1248 (1996).

[95] A. Feltrin and S. N. Cesaro, High Temp. Mater. Sci. **35**, 203 (1996).

[96] N. S. Loktyushina and A. A. Mal'tsev, Russ. J. Phys. Chem. **58**, 1602 (1984).

[97] N. S. Loktyushina, S. A. Zaitsev, S. B. Osin, and V. F. Shevel'kov, Vest. Mosk. Univ. Ser. 2 Khim. **42**, 434 (1987).

[98] Y. Q. Jia and S. G. Zhang, Inorg. Chim. Acta **143**, 137 (1988).

[99] R. D. Wesley and DeKock, J. Chem. Phys. **55**, 3866 (1971).

[100] J. W. Hastie, R. H. Hauge, and J. L. Margrave, in *Spectroscopy in Inorganic Chemistry*, edited by C. N. R. Rao and J. R. Ferraro (Academic, New York, 1970), p. 57.

[101] J. W. Hastie, P. Ficalora, and J. L. Margrave, J. Less-Comm. Met. **14**, 83 (1968).

[102] C. Gietmann, K. Hilpert, and H. Nickel, Internal Report JUEL-3337, Forschungszentrum, Jülich, 1996.

[103] C. W. Struck and A. E. Feuersanger, High Temp. Sci. **31**, 127 (1991).

[104] K. Hilpert, M. Miller, and F. Ramondo, J. Chem. Phys. **102**, 6194 (1995).

[105] A. Kovács, J. Mol. Struct. **482–483**, 403 (1999).

[106] A. Kovács and R. J. M. Konings, in *Handbook on Physics and Chemistry of Rare Earths*, edited by K. A. Gschneider, Jr. and L. Eyring (Elsevier, New York, 2003), Vol. 33, Chap. 213, pp. 147–247.

[107] D. Hegarty and M. A. Robb, Mol. Phys. **38**, 1795 (1979).

[108] K. Ruedenberg, M. W. Schmidt, M. M. Dombek, and S. T. Elbert, Chem. Phys. **71**, 41 (1982).

[109] S. R. Langhoff and E. R. Davidson, Int. J. Quantum Chem. **8**, 61 (1974).

[110] J. A. Pople, M. Head-Gordon, and K. Rachavachari, J. Chem. Phys. **87**, 5968 (1987).

[111] A. D. Becke, Phys. Rev. A **38**, 3098 (1988).

[112] J. P. Perdew, K. Burke, and M. Ernzerhof, Phys. Rev. Lett. **77**, 3865 (1996).

[113] J. P. Perdew and M. Ernzerhof, J. Chem. Phys. **105**, 9982 (1996).

[114] L. Joubert, G. Picard, and J. J. Legendre, J. Alloys Comp. **275−277**, 934 (1998).

[115] G. Lanza and I. L. Fragala, J. Phys. Chem. A **102**, 7990 (1998).

[116] A. Lesar, G. Muri, and M. Hodošček, J. Phys. Chem. A **102**, 1170 (1998).

[117] N. I. Giricheva, E. Z. Zasorin, G. V. Girichev, K. S. Krasnov, and V. P. Spiridinov, Izv. Vyssh. Uchebn. Zaved., Khim. Khim. Tekhnol. (Russian) **20**, 284 (1977).

[118] Y. S. Ezhov, S. A. Komarov, and V. G. Sevast'yanov, J. Struct. Chem. (Engl. Transl.) **41**, 593 (2000).